Unclassified

High-Power Tube Program

Semiannual Technical Summary Report to the Advanced Research Projects Agency

30 June 1961

Lincoln Laboratory
Massachusetts Institute of Technology

Unclassified

MASSACHUSETTS INSTITUTE OF TECHNOLOGY
LINCOLN LABORATORY

HIGH-POWER TUBE PROGRAM
SEMIANNUAL TECHNICAL SUMMARY REPORT
TO THE
ADVANCED RESEARCH PROJECTS AGENCY

30 JUNE 1961

ISSUED 24 JULY 1961

The work reported in this document was performed at Lincoln Laboratory, a center for research operated by Massachusetts Institute of Technology; this work was supported by the U.S. Advanced Research Projects Agency, Order No. 85-61, under Air Force Contract AF 19(604)-7400.

LEXINGTON MASSACHUSETTS


BLANK PAGE

TABLE OF CONTENTS

I. INTRODUCTION

The high-power tube program* was established to investigate some of the basic problem areas involved in the generation of high power. The projects that are currently active are reported in detail in the body of this report, and in summary in this introduction.

Work on klystron analysis has been concerned primarily with experimental verification of the theory. Generally good agreement between theory and experiment has been obtained. The effect of body-cooling water on output phase has been noted.

Preliminary results obtained with the beam pulse heating tube indicate an unexpected, but in retrospect reasonable, surface temperature function when the surface is heated with a pulsed electron beam.

Beam study work has continued to be concerned with the electrolytic tank and computer facility. The biased collector work has been hampered by brazing problems that were solved only when a pit-type hydrogen furnace was built and placed in operation.

Vacuum work carried on as a part of the cathode project has shown the reason for discrepancies noted in ion gauges operated under varying conditions. A cryogenic pumping system has been constructed for use with this project.

The secondary emission work has been completed and a report is in preparation. The effects of hydrogen firing, magnetic field, angle of incidence, and electron bombardment on the secondary emission ratio (δ) of a number of materials having a maximum δ less than one have been measured.

A technique for measuring loss distribution in RF cavities has been established. The experimental work is nearly complete; a report is in preparation. A note on the theoretical bandwidth of klystron output cavities has been prepared.

The small amount of work done on voltage breakdown has been concerned with surface cleaning and conditioning.

---

*This research is a part of PROJECT DEFENDER, sponsored by the Advanced Research Projects Agency, Department of Defense.

Duplexer investigations have been concerned with window materials, pressure-measuring techniques, and the use of a hot cathode electron source to provide a more reliable and rapid breakdown of the TR tube. Tests of a new L-band duplexer indicate good performance at 10-Mw peak, 25-kw average. Tests at higher power are planned.

A paper on high-power duplexers was presented at the IRE 1961 National Microwave Symposium.

R. C. Butman

II. HOLLOW BEAM – KLYSTRON INTERACTION

This work is being carried on under Subcontract No. 225 by Varian Associates.* The program was established to investigate the use of high-perveance hollow beams in high-power wide-band klystrons.

The second six-cavity klystron using a high-perveance magnetron injection gun to produce a hollow beam has been operated. After several unfortunate accidents with the tube, significant data have been obtained during the last two months. There has not yet been opportunity for extensive analysis of these data. However, some tentative qualitative conclusions may be drawn at this time.

A. SMALL SIGNAL REGIME

Linearity:– It appears that linear small signal conditions in the beam hold only up to gap voltages of about 20 per cent of full beam voltage (V_o). For example, the beam-loaded Q measured on a cavity for which the gap voltage is varied stays constant to about 1/5 of V_o and then the Q decreases monotonically to about 1/2 the original Q by the time RF gap voltage equals V_o. Within the linear region, however, present methods of calculating electronic loading and gap-to-gap transconductance appear to be valid as long as the space-charge potential depression of the beam in the gap is taken into account.

Noise:– Measurements made on a two-cavity experiment with essentially the same beam are reported in the last Quarterly Report of 1960 on Subcontract No. 225 (received from Varian since 31 December 1960). These measurements show noise peaks that are voltage- and magnetic field-tunable, superimposed on a white noise background. The noise power becomes noticeable in the region of 20 kv and is about 5 orders of magnitude greater than shot noise at the nominal values of operating voltage and field (i.e., about 45 kv and 1200 gauss).

* For an outline of the aim and status of the experiment prior to 31 December 1960, see Reference 1.

B. LARGE SIGNAL REGIME

The present six-cavity tube has a gun anode that is insulated for moderate voltage from the body of the tube. This configuration allows the beam voltage to be held constant and the magnetic field and perveance to be adjusted independently. Driving the first cavity and sampling the current at the second cavity gap has shown that, in the range of 6.5- to 10-μ perveance, the ratio of RF beam current to DC beam current (I_o) decreases with increasing perveance. It has also shown that, for fixed beam voltage (45 kv), the RF current-to-I_o ratio increased with increasing magnetic field in going from about 950 gauss up to about 1200 gauss, at which point the RF current leveled off. It was also observed, by sampling the current at the third gap and driving the first gap, that the remodulation at the second gap was not as effective in producing saturated current at the third gap as the direct drive at the first gap was in producing saturated current at the second gap (i.e., $I_3 \simeq 2/3\ I_2$). This statement is, of course, true for a particular circuit arrangement where the drift lengths are equal to each other and equal to about 90° of the DC beam plasma wavelength, and where the gap lengths are relatively long (about 1-1/2 radians). In a sense, however, it is typical of most of the large signal observations on this tube to the extent that current saturation is observed for significantly shorter transit angles (measured in terms of the usual DC beam properties) than has been observed in the case of lower perveance beams. It is believed that this saturation is related to an effective increase in instantaneous beam plasma frequency in the bunch at high space-charge density in general, and in the gap in particular, because of the increased space-charge potential depression.

This subcontract will terminate with the completion of measurements on the present tube and the issuance of a final report.

G. L. Guernsey

III. MULTICAVITY KLYSTRON ANALYSIS

A series of gain and relative phase measurements on multicavity klystrons has been started. These measurements are intended to evaluate the small signal, space charge wave analysis of klystron interaction that we have programmed for digital computation. They are also intended to define the phase-frequency limitations of klystrons for use in pulse compression systems.

The initial evaluation is being performed on a VA-87-C, 4-cavity pulsed klystron with a nominal peak output power in the 1- to 2-Mw range and a synchronously tuned gain of about 68 db.

Preliminary results of these experiments indicate the following:

(1) The phase tuning of such a tube by variation in coolant water input temperature may be as large as thirty degrees electrical tuning for a 10°F change in temperature where the phase-frequency slope is about 14°/Mcps. Although this is an extreme case, it advises caution in the application of such tubes to parallel operation.

(2) The measured maximum gain is within about 1 db (low) of the calculated maximum gain over a range from 50 to 68 db (depending on the degree of stagger tuning). This gain comparison is illustrated in Figs. III-1 and III-2, which show the synchronously tuned gain and a case of stagger tuning, respectively. The slight displacement in frequency of the two curves of Fig. III-1 (~0.05 per cent or 1.5 Mcps) is probably accounted for by the fact that the analysis uses zero reactive component of the circuit admittance as the criterion for tuning to a given frequency, while the experiment uses maximum output at that frequency as the criterion for tuning the circuit to a frequency.

(3) The gain vs frequency for stagger tuning shows a more rapid decrease in gain for high frequencies than that predicted by the analysis. This discrepancy can be seen in Fig. III-2, for which cavity 2 is detuned −1 per cent and cavity 3, +1 per cent from center frequency. At this time there is insufficient data to make it possible to determine whether the difference represents a deficiency in the theory or is a result of not reproducing exactly in the experiment the conditions specified in the analysis. However, measurements of the output circuit pass characteristic show that the assumption used in the calculation of

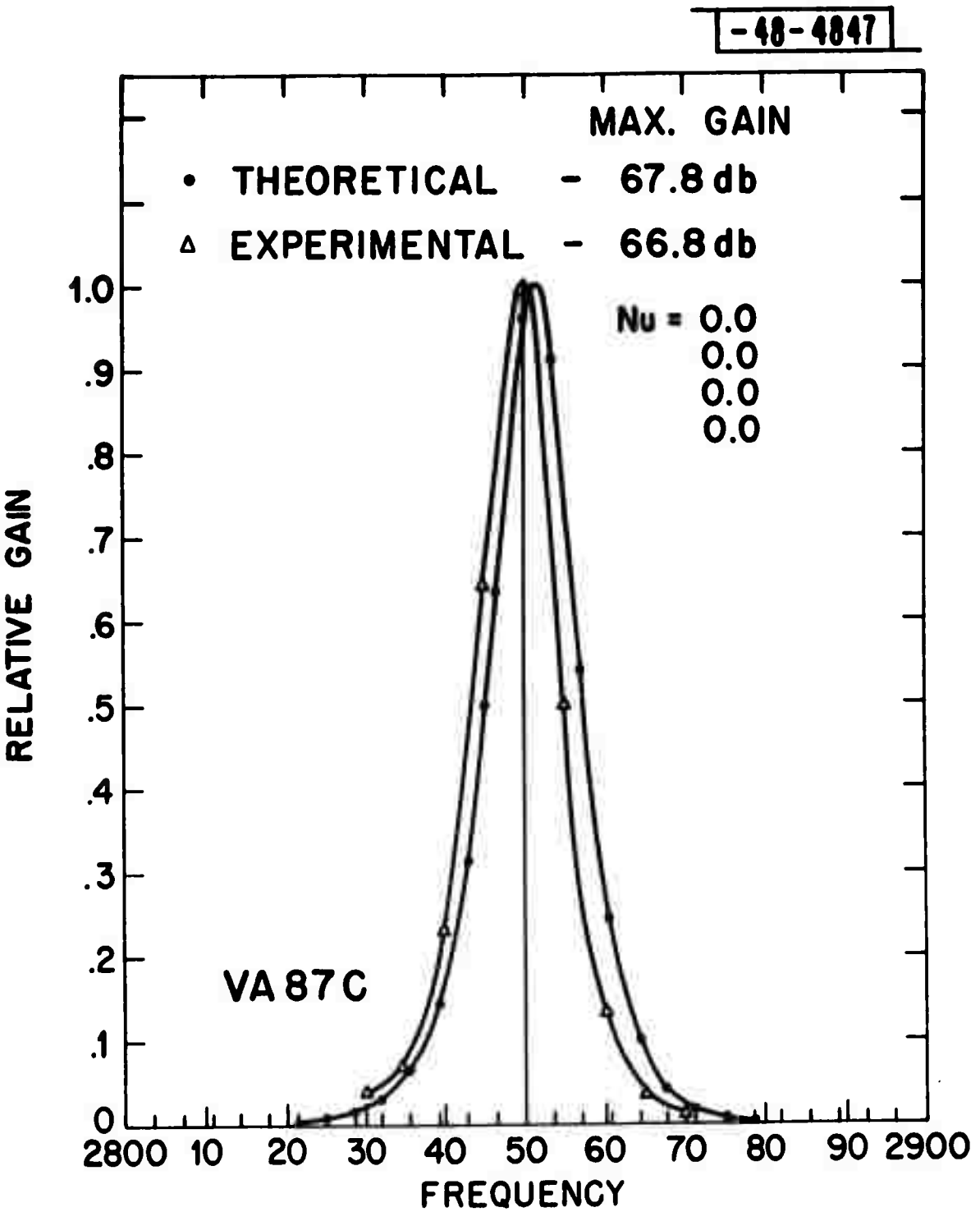

Fig. III-1. Klystron gain vs frequency (synchronous tuning).

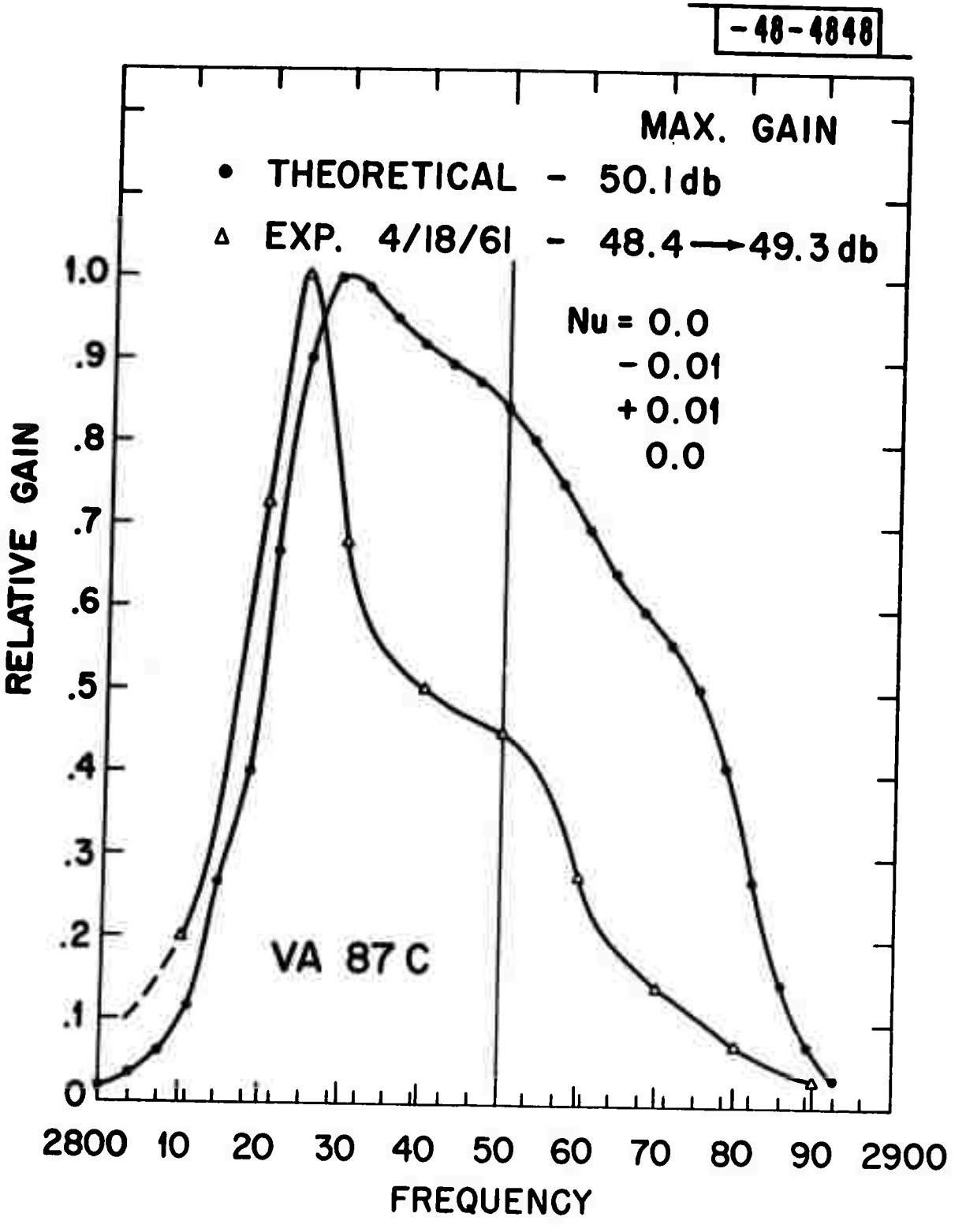

Fig. III-2. Klystron gain vs frequency (stagger tuning).

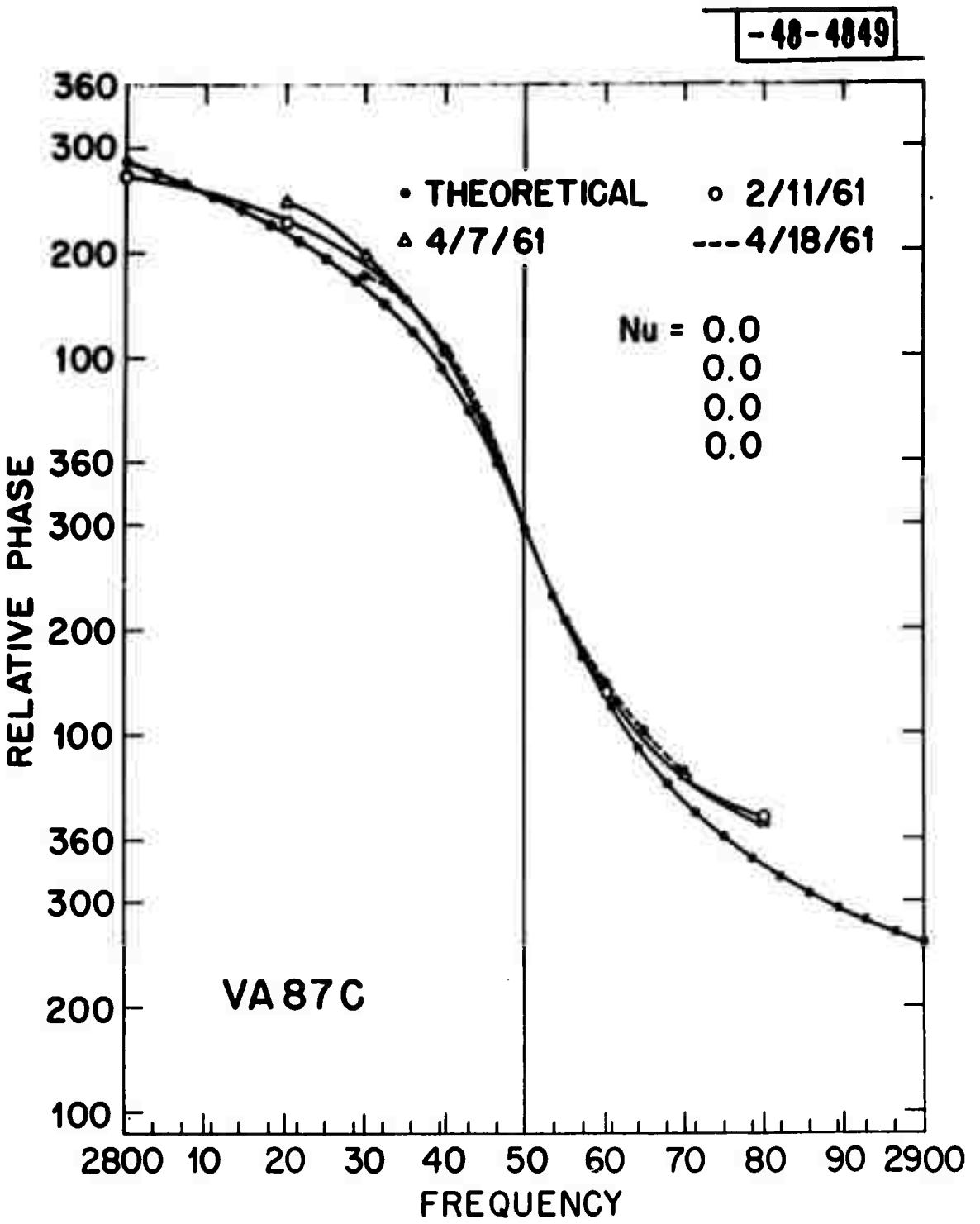

Fig. III-3. Klystron phase vs frequency (synchronous tuning).

a single tuned resonance shape is not justified. These data, although not yet reduced to an appropriate correction, do appear to account for at least part of this high frequency fall off.

(4) The experimental values of phase-frequency response agree with the computed values for synchronous tuning and two cases of stagger tuning to within the present experimental accuracy (±3°). The raw data of phase-vs-frequency are shown in Figs. III-3 and III-4, compared with the calculated relative phase. These data are for the same cases of synchronous and stagger tuning for which the gain is given in Figs. III-1 and III-2, respectively. The gross skewing of the measured curves with respect to the calculated curves results from not applying the correction due to phase variation of a variable attenuator. It is desirable to reduce the experimental error to less than ±1°, and such a reduction seems possible. Work is continuing on improving the accuracy of the experiments and on resolving the remaining discrepancy between theory and experiment.

G. L. Guernsey

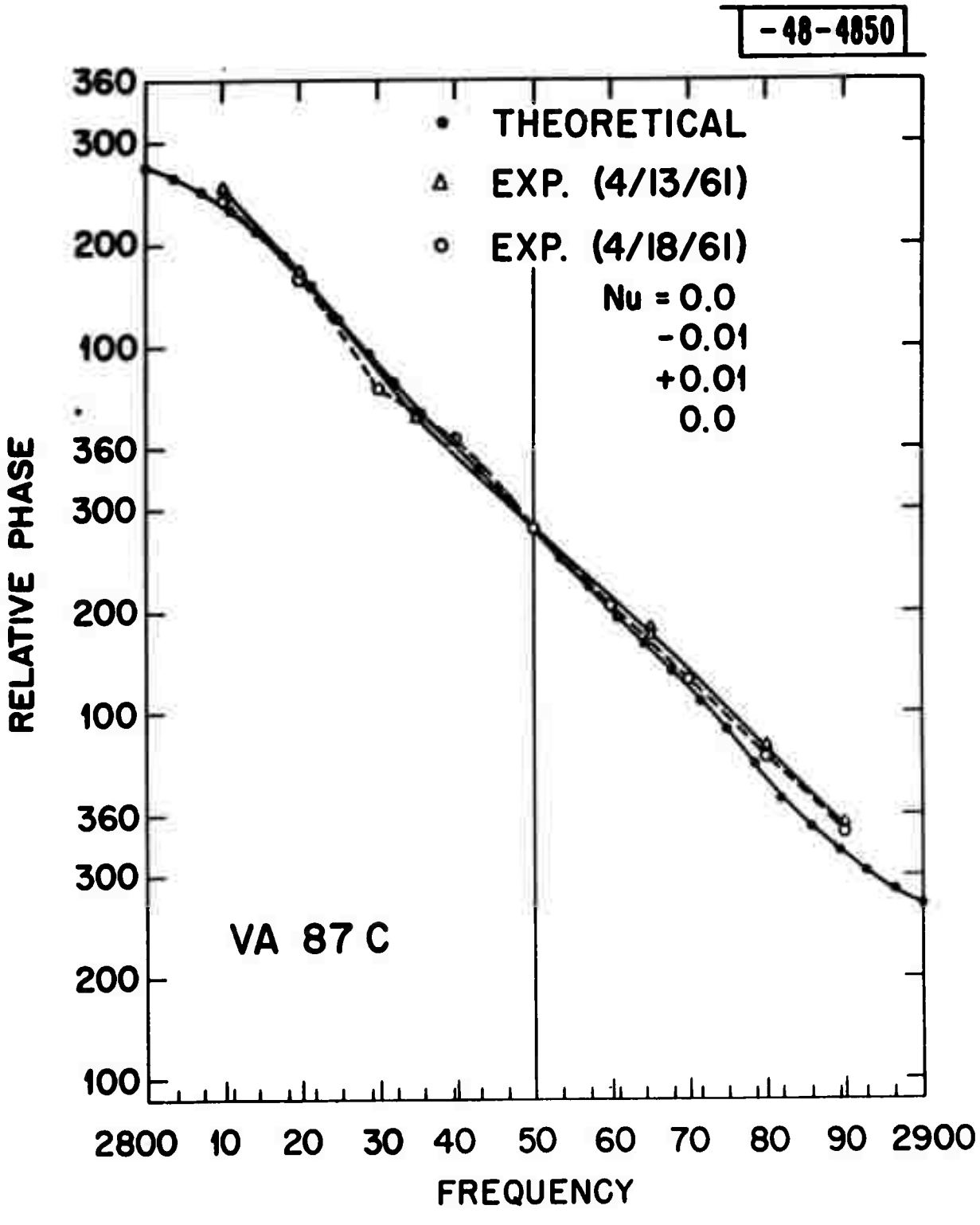

Fig. III-4. Klystron phase vs frequency (stagger tuning).

IV. BEAM PULSE HEATING

This program was set up primarily to measure the instantaneous surface temperature and rates of evaporation of metallic surfaces subjected to high-intensity pulsed electron beam bombardment. The metallic vapors that are liberated from these bombarded areas may be deposited on critical surfaces within a high-power microwave tube and thereby limit its peak power output. Experiments are under way to measure the rates of evaporation for copper and other materials under various conditions of pulsed operation so as to establish the limits of peak power that can be absorbed without destructive effects.

During the past reporting period, the beam pulse heating tube (XT455) described in the last Semiannual Report,[1] has been processed and pulsed to 80 kv. During the initial processing of the tube, the glass bellows connecting the tube manifold to the diffusion pump broke, and the tube was let down instantly to atmospheric pressure while at a temperature of 425°C. At this temperature and pressure, the copper and stainless-steel surfaces within the tube became heavily oxidized. The decision was made to reprocess the tube even though it was almost certain that the cathode surface had been poisoned and that reprocessing at 425°C would not completely remove all the oxide film. We could not expect to operate this tube at the rated 10 Mw/cm^2 beam power density; however, data that we could obtain at the reduced beam power densities would be useful in evaluating our instrumentation and associated equipment.

The XT455 was installed in the high-voltage tank assembly and pulsed up to 80 kv. As anticipated, the tube was gassy and its measured perveance was low (1.1×10^{-6} instead of 1.8×10^{-6}). At pulse voltages above 60 kv, internal breakdown occurred between cathode and anode. Cathode emission was limited to approximately one-half rated current even at 1-1/2 times rated input filament power. A few volts applied to the filament resulted in a change of two orders of magnitude in tube pressure as recorded by the Varian pump on the tube manifold. A degassing time of at least two hours was always required for the tube pressure to stabilize at a safe operating level. One is led to the

Fig. IV-1. Photograph of the TiB_2 surface during single pulse (10-μsec duration) bombardment.

conclusion that water vapor was present within the tube and released from the cathode surface when filament power was applied.

The tube incorporated three OFHC copper targets and one TiB_2 target. The TiB_2 target was installed so that initial beam studies could be made prior to the actual bombardment of the copper targets. The melting temperature of TiB_2 is 3000°C, compared to 1080°C for copper. The TiB_2 target consisted of 0.020 in. of TiB_2 deposited by plasma torch on a 0.125-in. OFHC copper plate. All experiments were conducted with this target.

Approximately 3810 single pulses of 10-μsec duration were applied to the TiB_2 target. During single-pulse operation of the tube, the surface heating was very intense and produced a very bright spot on the target. A photograph of the light produced during a single impulse is shown in Fig. IV-1. Also seen on the same photograph is the light reflected from the stainless-steel shield surrounding the target and from the two steel screws that secure the target to the collector assembly. The tube was pulsed at 55 kv peak voltage, 12 amperes peak target current and 2.1 Mw/cm^2 peak beam power density. A magnetic field of 590 gauss was required to focus the beam to the 1/4-in. diameter.

A photograph of the target is shown in Fig. IV-2. One can clearly discern the area at which bombardment and evaporation of the TiB_2 took place. The total reduction in weight of the target resulting from the pulsed bombardment was 0.0064 gm. The initial weight before bombardment was 20.1617 gm.

The surface-temperature rise was monitored by a photoelectric pyrometer. The pyrometer uses a telescope modified to receive an RCA 7102 photomultiplier tube whose spectral response covers the range from 4200 to 11,000 Å. The bombarded area is viewed through the pyrometer eyepiece and focused by the telescope objective lens. The photomultiplier tube is mounted at 90° to the axis of the telescope. Radiant energy passing through the objective lens is deflected onto the cathode of the photomultiplier tube by a mirror mounted internally at 45° to the telescope axis. The photoelectric pyrometer was viewed on an oscilloscope. The measured response time of the photoelectric pyrometer was less than 0.3 μsec.

The instantaneous temperature measured at the surface of the TiB_2 target for a single pulse is shown in Fig. IV-3. The observed temperature rise and

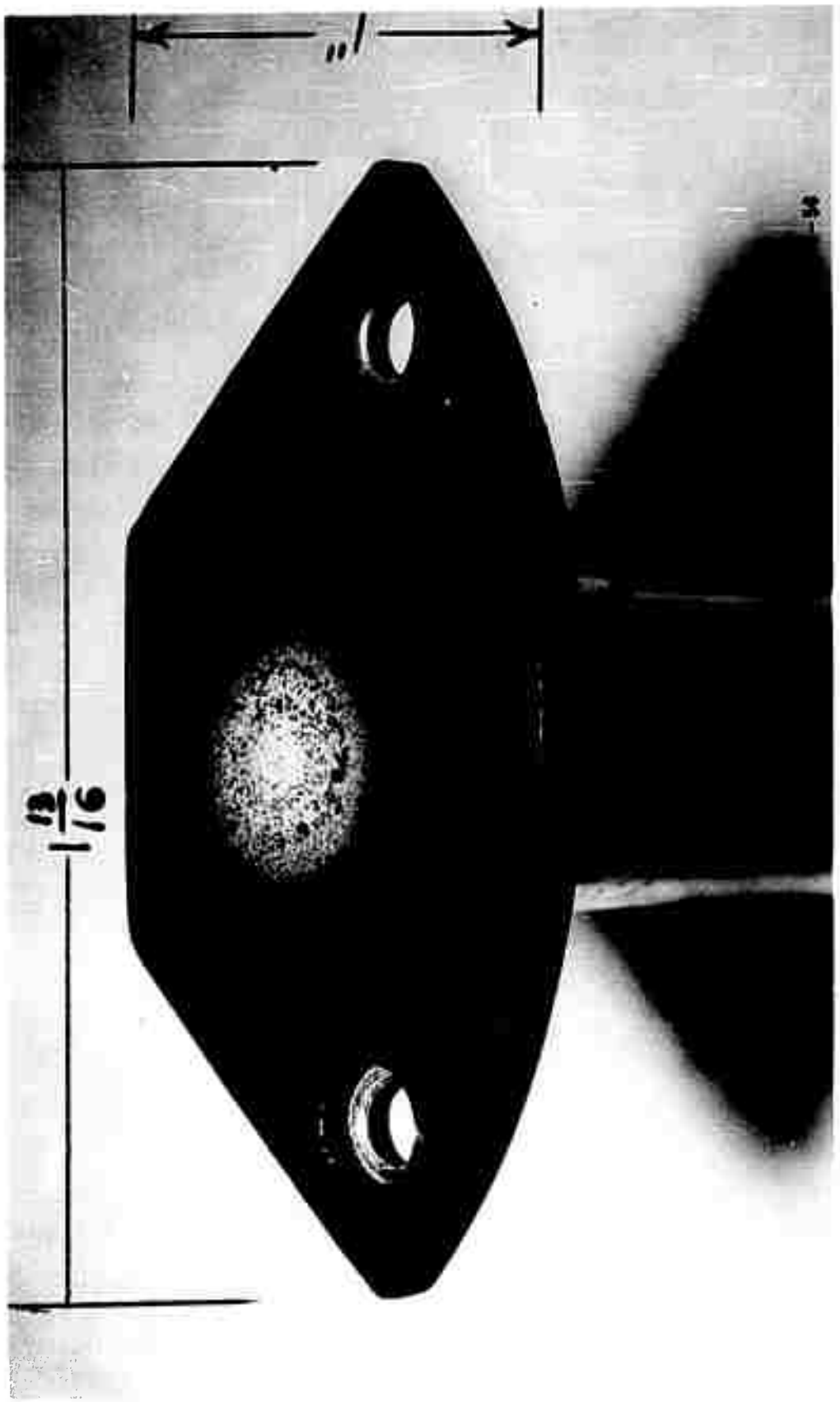

Fig. IV-2. Bombarded TiB_2 target.

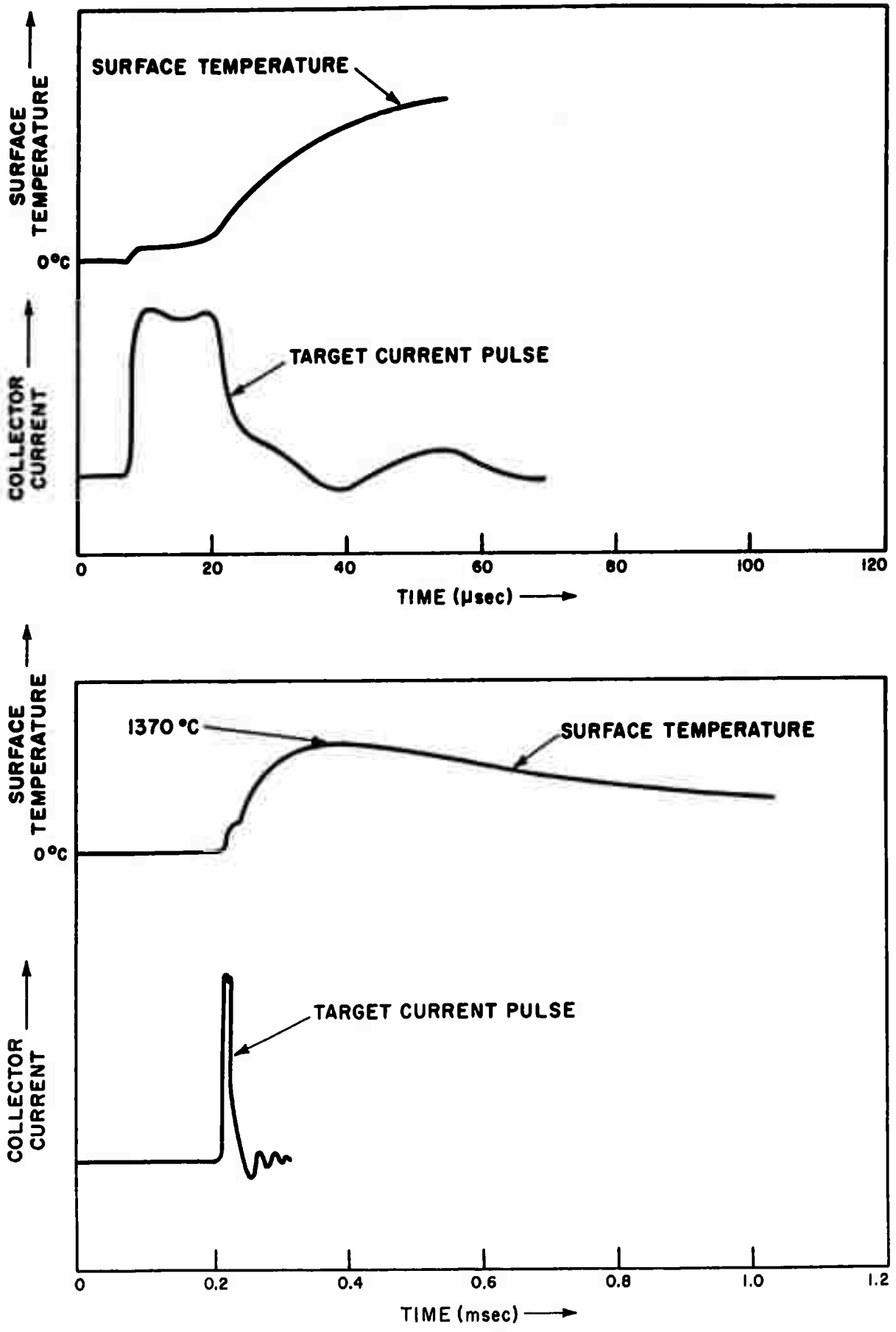

Fig. IV-3. Instantaneous temperature at surface of TiB_2 target vs time.

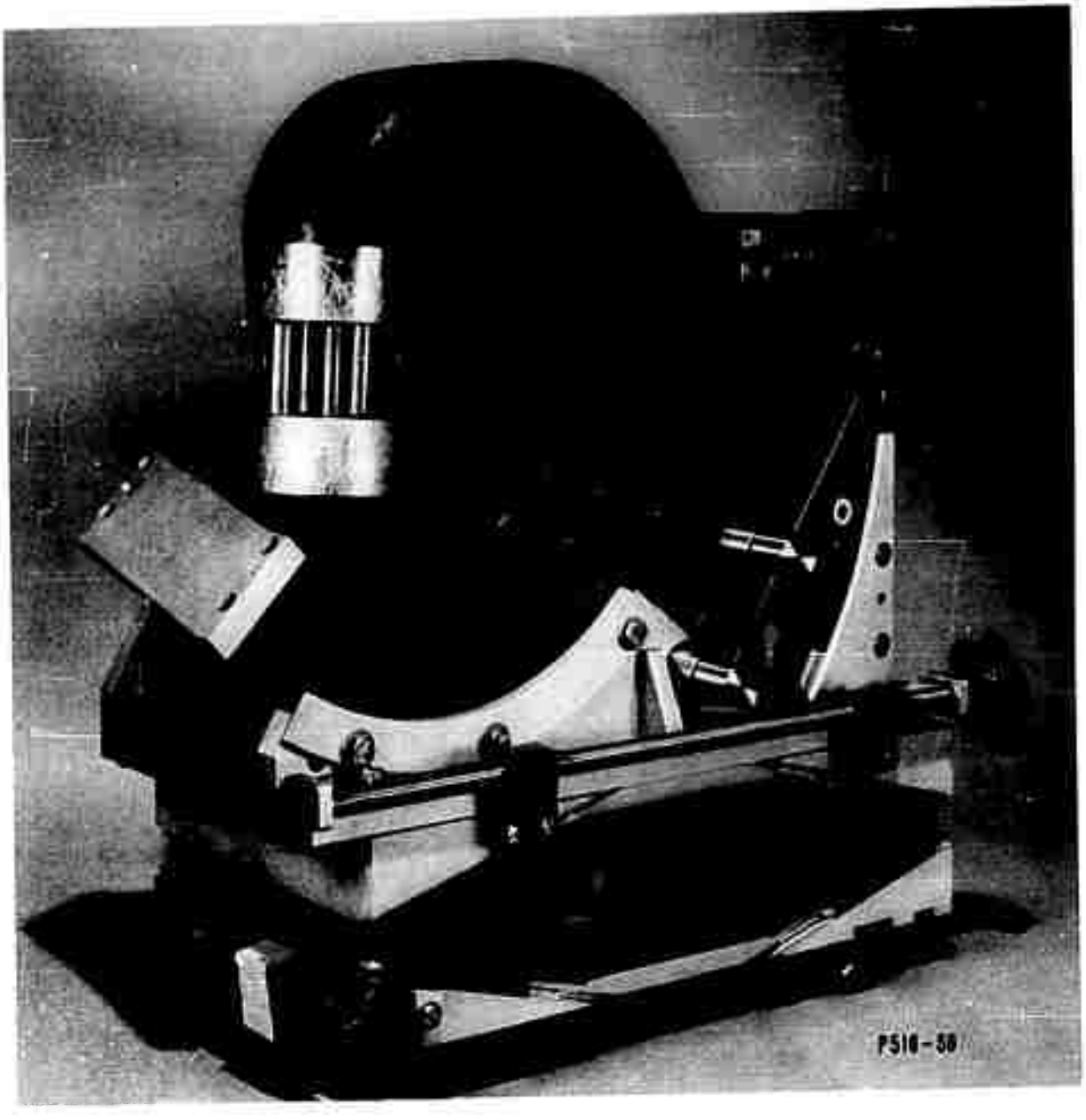

Fig. IV-4. Omegatron magnet mount.

target current pulse have been plotted on the same time scale. From the two top graphs, one observes that there is a relatively low temperature rise on the target surface during the pulse duration and that the surface temperature continues to rise long after the end of the pulse. As seen from the two bottom curves, the temperature reaches a maximum value of 1370°C approximately 12 pulse durations after the end of the current pulse.

There are two comments to be made on these preliminary observations: (1) The maximum temperature measured agrees with the order of magnitude of temperature predicted on the basis of a simple model of beam penetration for the voltage and power density used (although the measured value appears low). (2) That the maximum temperature does not appear until after the beam pulse is terminated is consistent with the fact that a maximum rate of energy loss with depth actually occurs below the surface at a depth of the order of 0.001 in. This circumstance, then, introduces a delay in the time at which maximum surface temperature appears. The low thermal conductivity of TiB_2 probably accounts for the fact that the time constant of this delay is as long as is indicated (of the order of the pulselength in this case).

All components for XT455 serial 2 have been fabricated and tested. It is expected that the second beam pulse heating tube will be ready for experimental evaluation before the end of July.

No additional measurements were made on the omegatron mass spectrometer during this reporting period. The adjustable mount required for the omegatron was completed and is shown in Fig. IV-4. Rotational motion in two planes and linear motion in two additional planes are accomplished by adjusting the four knobs shown in the photograph. Extremely small incremental variations in magnet position are required for optimizing the electron current in the omegatron tube.

E. Silverman

BLANK PAGE

V. BEAM STUDIES

The construction of the electrolytic tank setup that will be used for the high-power electron beam design studies is in its final stages. A Benson-Lehner x-y-plotter was used to provide the traverse system for the probe pickup.[1] A desk-type analogue computer will serve as a differential analyzer for the system. The frame of the plotter is big enough to allow us to use an electrolytic tank four-by-five feet in size. The tank and the frame of the plotter are mounted on the same welded aluminum frame. A four-screw adjustment is provided for the leveling of the pickup probe traverse system with respect to the electrolyte level in the tank. Figure V-1 shows the x-y traverse system, the aluminum supporting frame and the tank.

The electrolytic tank itself is provided with a tilting plane so that beam design studies can be made for electron devices in the rectangular coordinate system as well as for problems involving cylindrical symmetry. At first, it was decided to use a tilting plane made of lucite. The use of a plane made of this plastic material has many advantages, the most important of which are its machinability and its resistance to breakage as, for example, compared to glass. However, after consultation with some people familiar with plastics, it was decided to use a plane made of aluminum spray-coated with plastic, because it was feared that the lucite plane would deform under the weight of electrodes and as a result of aging of the plastic. The reinforced aluminum plane is now completed and exhibits a very plane surface of hard, settled plastic. Figure V-1 shows a part of this tilting plane in the electrolytic tank.

Figure V-2 shows the pickup probe, made demountable to accommodate different pickup points, one of which is shown to the right of the probe. The probe can be adjusted both horizontally and vertically. A micrometer screw will make the vertical adjustment very accurate. The box next to the probe holder will contain preamplifiers for the pickup probes.

In order to be able to plot equipotential lines or electron trajectories, an x-y plotting system is necessary. After a study of commercially available plotting equipment from the point of view of size, accuracy and cost, it was

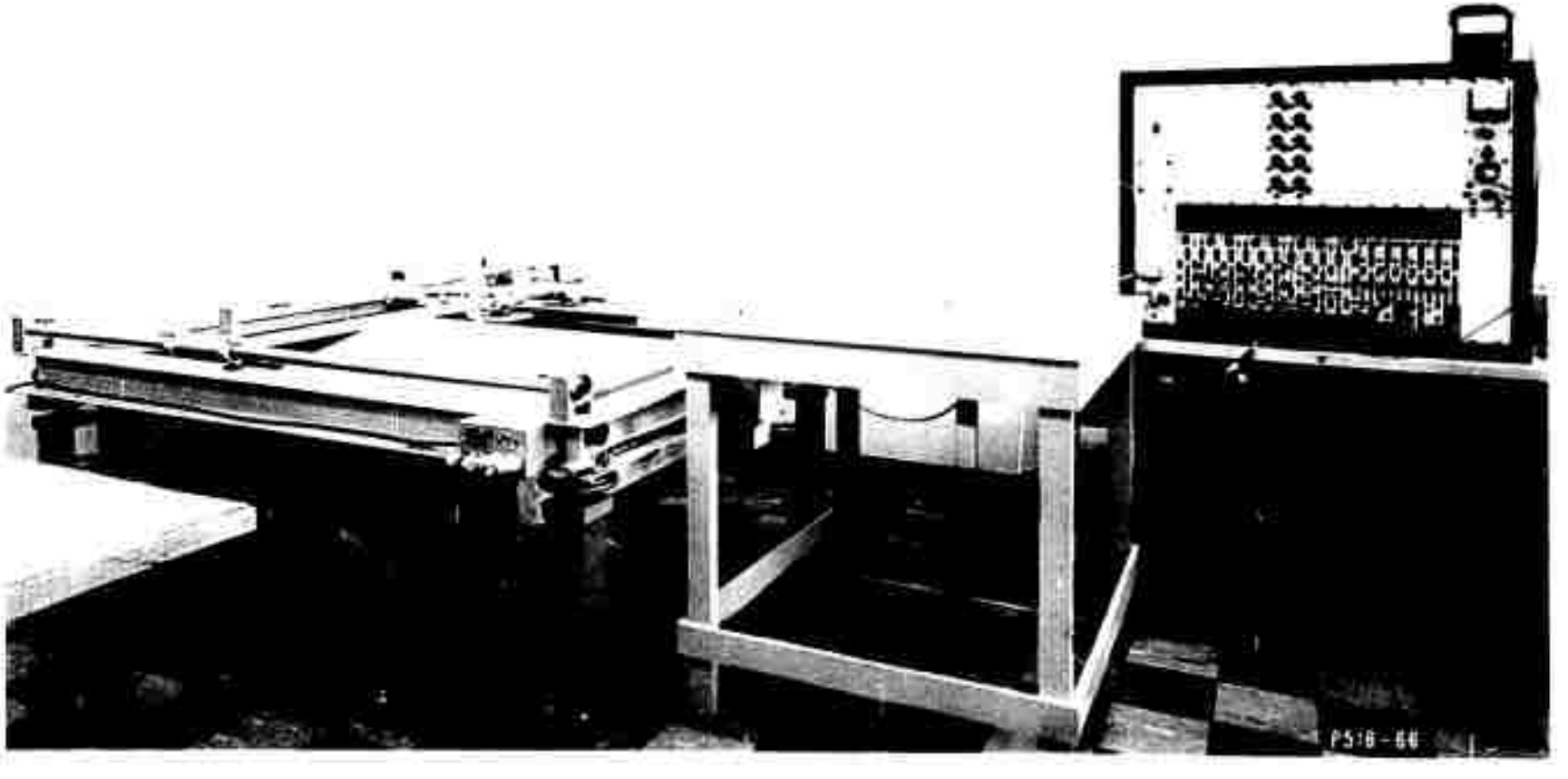

Fig. V-1. Electrolytic tank setup.

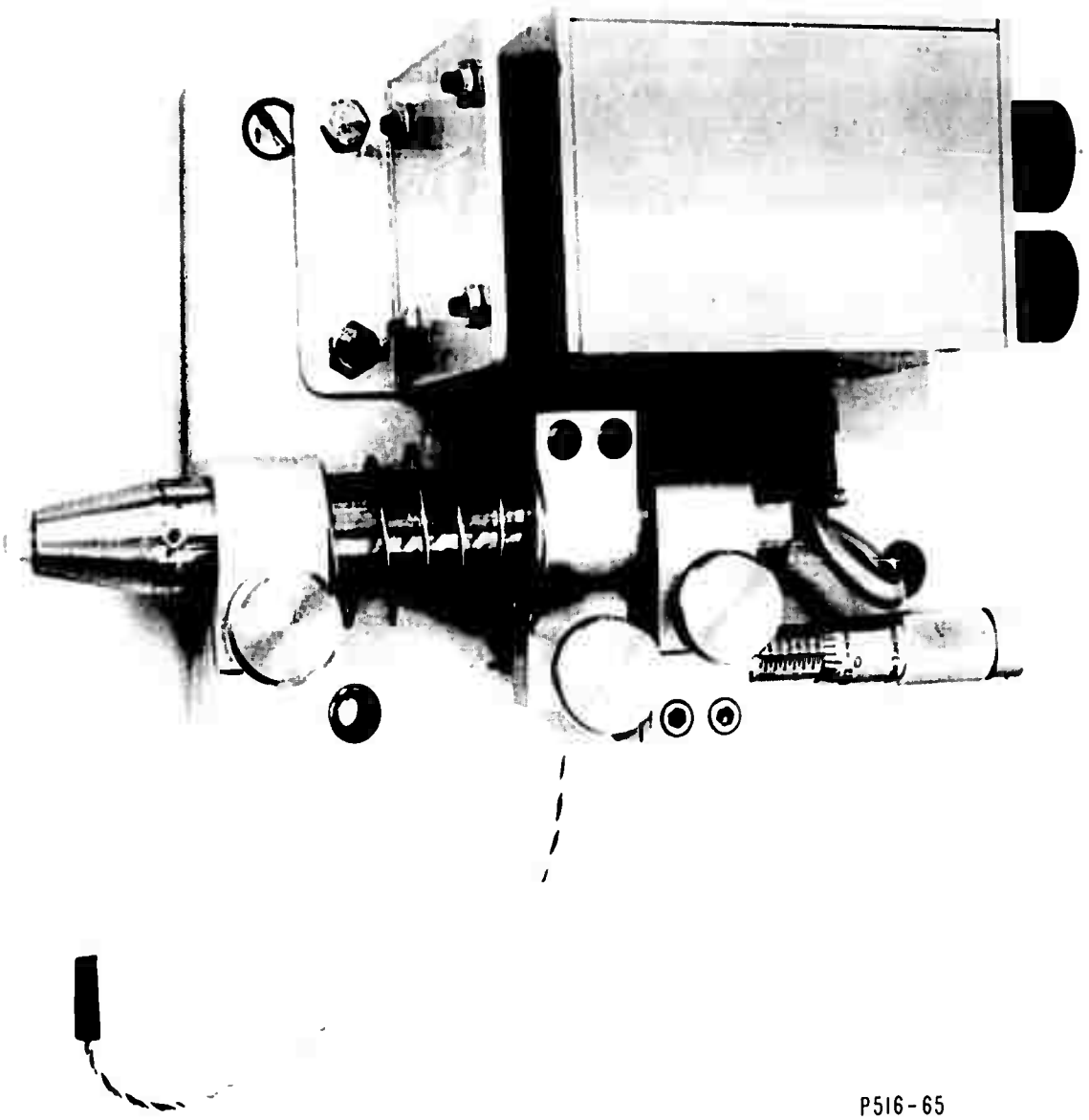

P516-65

Fig. V-2. Probe assembly shown with an extra probe.

decided to build a pantograph and make the plot of the excursion of the probe through a mechanical linkage between the pen and the probe. This pantograph is shown mounted on the system in Fig. V-1. It offers a four-to-one area reduction.

In Fig. V-1, one can also see the differential analyzer made by Applied Dynamics, Inc. This analyzer will be used to solve the equations of motion of the electrons in electromagnetic systems. It is a small, table-model, tube-type, analogue computer (model AD-1-32) comparable to equivalent commercial, transistor-type computers; however, according to the manufacturer, the component accuracy of this unit is better than 0.1 per cent. Some test solutions have been run on this computer and it was found that the equipment behaves satisfactorily. Accuracy tests of the computer are currently in progress.

The first use of the electrolytic tank setup will be for plotting equipotentials in some simple electromagnetic systems for the calibration of the system components. The next step will be to calibrate the system for tracing of electron trajectories. After this, the system will be used for the solution of actual beam problems.

A. Saharian

VI. BIASED COLLECTOR

As noted in previous reports, the biased-collector project has as a principal objective the study of the velocity spectrum of the spent beam of a klystron. Information obtained in this study is expected to be of value in assessing the practicability of biased collectors in general.

Construction difficulties have again delayed completion of the experimental unit being assembled for use with this project. Unsatisfactory performance by a subcontractor who had been given the responsibility of brazing insulator supports into the stainless-steel collector envelope resulted in the decision to construct the required pit furnace at Lincoln Laboratory. This furnace was designed and constructed during the first portion of the reporting period. Operation of the unit is satisfactory; with it the necessary brazes have been made on the collector envelope. Collector-segment insulators have been welded on and the entire unit has been found to be vacuum tight. The collector segments have been coated with titanium carbide in order to minimize their secondary emission ratio. The remaining construction operations involve heliarc welds of a standard nature. The equipment necessary for processing and testing the tube is available, and velocity spectrum measurements will commence as soon as construction of the tube is complete.

A. Saharian

BLANK PAGE

VII. CATHODES

The major effort to date has been concerned with establishing reliable vacuum techniques for our future cathode studies. There has been so much controversy in the literature that it seemed desirable to investigate some of the questions in order to establish techniques in which we could have confidence.

A major problem is the reliability of ionization gauges. Principally, since an ionization gauge acts as a pump, there is some question as to whether such a gauge mounted in a small enclosure and connected to a large vacuum chamber through a small tube really measures the pressure in the vacuum chamber, or something else proportional to that pressure, under varying conditions. The arrangement that we used to compare gauges is shown in Fig. VII-1. In this figure, BA is a conventional Bayard-Alpert gauge. Gauges N_1 and N_2 are Nottingham gauges.[2] (These gauges are made by adding a screen outside the normal Bayard-Alpert gauge, and maintaining it negative with respect to cathode. The screen repels electrons back toward the electron collector, thus increasing the probability of ionization, and hence increasing the sensitivity of the gauge. There is still another result that we shall mention later.) Of these, N_1 is in a conventional envelope connected by a small tube to the vacuum chamber, while N_2 is mounted directly in the chamber. With this arrangement, we could compare different gauges (BA and N_1) in the same environment (in small enclosures), and identical gauges (N_1 and N_2) in different environments. The second comparison is of interest because, even though it may seem evident that the ideal arrangement would use a gauge in the vacuum chamber, this is not always practical. The positive ion current to the ion collector in each gauge was measured, and the following current ratios computed: N_1/BA, and N_1/N_2. It was not considered necessary to relate the currents to known pressures (although BA had a nominal calibration which was used as a guide), and no import was attached to the magnitudes of the ratios, but variations in the ratios were considered significant since they revealed inconsistent behavior of one or both of the gauges concerned. Readings for which ratios were computed were all taken when all the gauges were operating simultaneously.

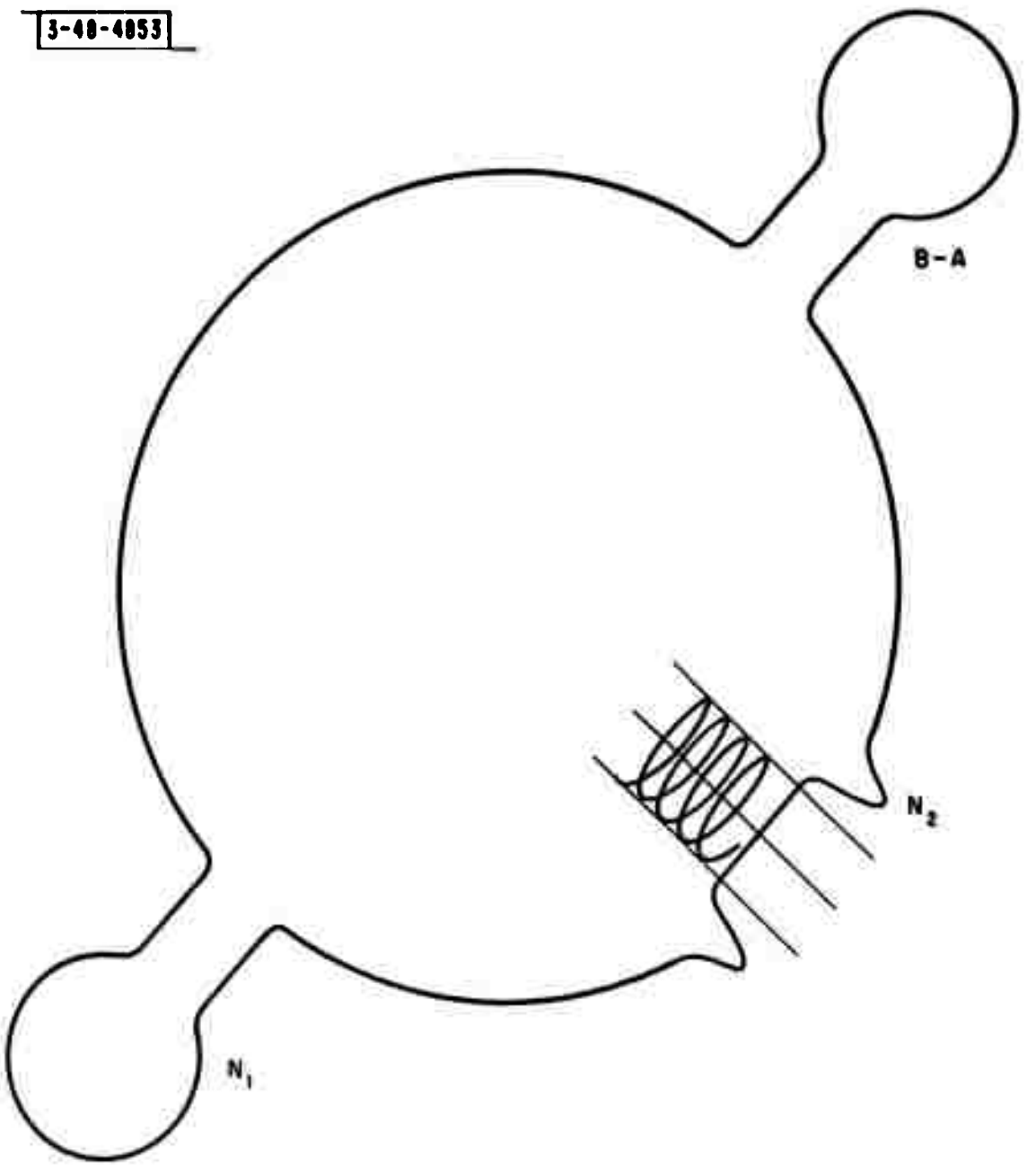

Fig. VII-1. Gauge test chamber.

In a series of measurements of the steady-state positive ion current, made while the system was being put into operation and tested, it was found that N_1/N_2 showed much less variation than did N_1/BA. Since the readings do not all refer to the same experimental conditions, it does not seem that a conventional statistical analysis would be valid; however, it does seem to be significant that of some 60 readings, 62 per cent of the values of N_1/N_2 were within ±10 per cent of the median value of 1.02, whereas only 21 per cent of the values of N_1/BA were within ±10 per cent of the median of 2.98. Further, the extreme range of the latter set was larger. These results seem to show that the Nottingham gauge is less sensitive to its environment than the Bayard-Alpert.

Measurements of the positive ion current vs time were made for periods up to 3 hours after the ion gauges were turned on. "Turning on" consisted of allowing the filament to run at the proper temperature (determined by previous trial) for 15 minutes, and then, at t = 0, turning on the electrode voltages. We found that, as we had expected, ion current decreases with time in a roughly exponential manner. This decrease is believed to be mostly, but not entirely, the result of the pumping action of the gauge, the effect of outgassing of the gauge being secondary. We also found that (a) N_2 reduces the pressure in its enclosure more slowly than N_1; (b) when N_1 and N_2 are both connected as Bayard-Alpert gauges, the same thing is true; (c) N_1 connected as a Bayard-Alpert gauge pumps more rapidly than N_1 with the regular connections; and (d) the same can be said for N_2 as a Bayard-Alpert gauge vs N_2 as a Nottingham gauge, although the difference is less in this case. (To make a Bayard-Alpert gauge, the screen is given a positive potential by connecting it directly to the electron collector.) Both (a) and (b) can result from the fact that N_2 is in a larger enclosure than N_1.

These results also show that the pumping is done by the gauges, not by the diffusion pump; if it were done by the latter, our turn-on effects would have been interchanged, N_2 being closer to the pump than N_1. Result (c) indicates that the wall of the gauge enclosure is involved in the pumping, since in N_1 the electrons are kept within the screen. The effect is less pronounced in (d), since in that case the wall is more remote in N_2 and has less effect in the

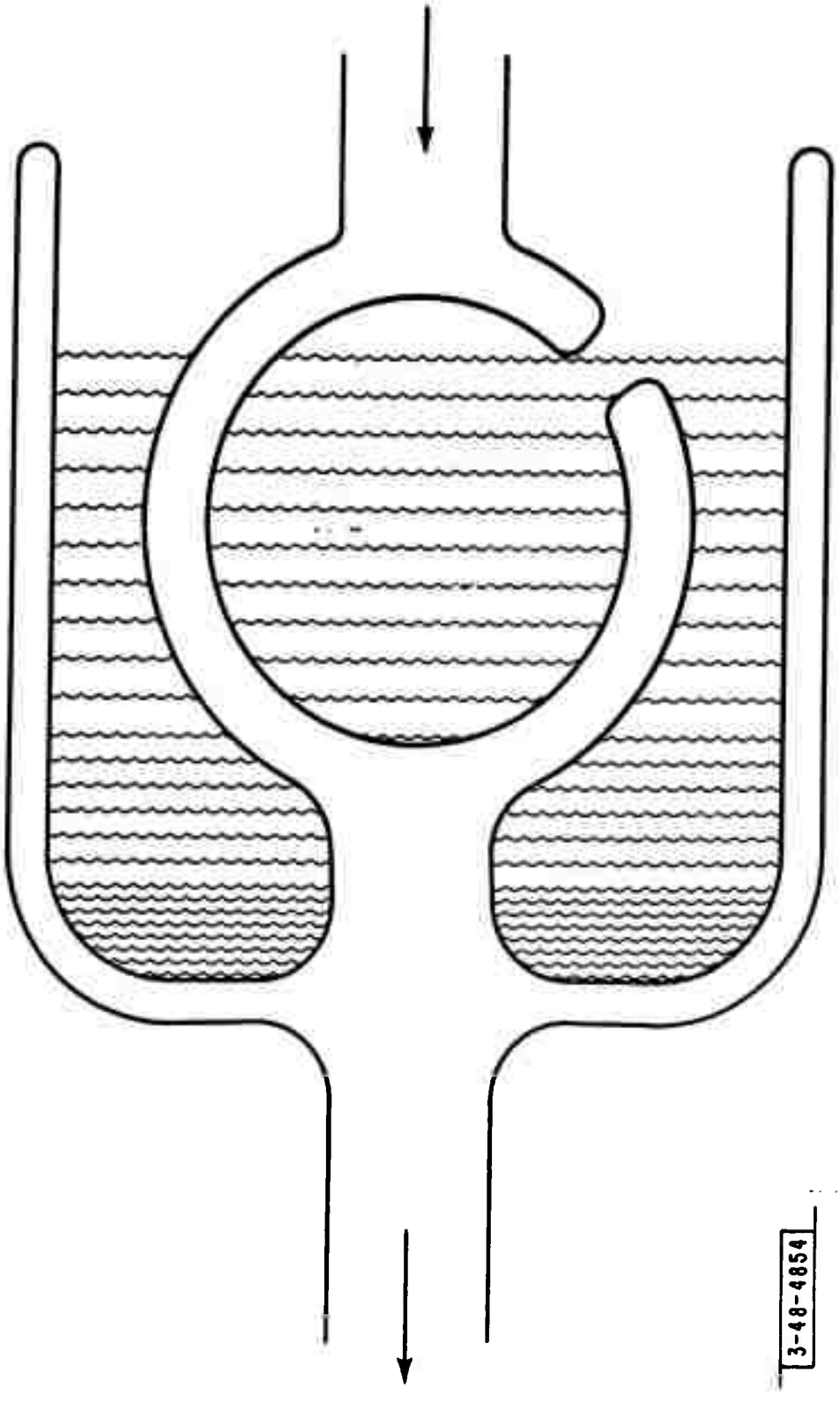

Fig. VII-2. High-speed trap.

Bayard-Alpert case. Results (c) and (d) agree in general with measurements on the regular Bayard-Alpert gauge. Turn-on measurements on the latter are not quoted here, because its enclosure and connection to the main chamber were different enough to cast some doubt on the validity of a comparison.

The results discussed above were obtained when the system was contaminated with oil vapors from the pump. Earlier measurements of the turn-on effect in a clean system at a lower pressure showed that (a) the effect was much smaller in all gauges; (b) a steady state was reached much sooner; and (c) gauges N_1, N_2 and BA agreed much more closely with one another.

In one experiment, the three gauges were operated continuously while the liquid nitrogen was allowed to evaporate from the cold trap and readings were taken. The construction of the trap is shown in Fig. VII-2. In Figs. VII-3(a) to VII-3(c) are shown graphs of (a) the positive ion current for one of the gauges, (b) the variations of N_1/N_2 and BA/N_2, and (c) the liquid level in the trap. All are referred to the same time axis. Only one curve is plotted in (a), since all three had much the same shape, and differences between them were not obvious. In (c) we chose to plot BA/N_2 rather than the ratio N_1/BA that we used formerly, because the previously discussed measurements led us to believe that N_2 was the most reliable comparison gauge, and our results are more easily interpreted in this way. The ratio BA/N_2 was normalized to match N_1/N_2 at the first reading.

Looking at the first graph (3a), we see that, before the time marked by the first arrow, events of only minor interest (probably connected with stabilizing of the gauges) occurred. It is worth noting, however, that the Bayard-Alpert gauge seems to be less steady than the others. At the time marked by the first arrow, the outer part of the trap emptied and there was a small burst of gas. The two Nottingham gauges continued to agree quite well with one another, though each was affected. The Bayard-Alpert gauge, however, deviated appreciably in its relative indications, as well as absolutely. At the second arrow, the pressure was starting to rise because of the warming of the inner trap surface, and at the third, the inner trap was empty. Such a large volume of gas was released that conditions were far from steady. It is quite probable

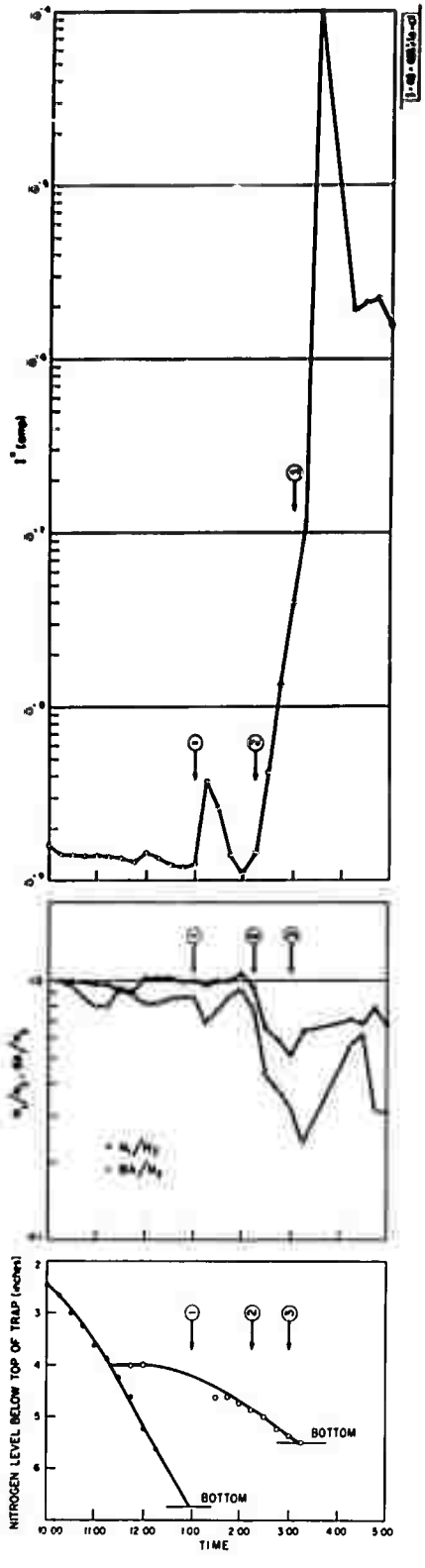

(a) Ion current vs time for N_2

(b) N_1/N_2 and BA/N_2 vs time

(c) Nitrogen level in trap vs time

Fig. VII-3.

that the pressure was higher at N_2 than at N_1, and that N_2 read higher than N_1 for this reason, exclusive of any possible difference in the pumping speed of the two gauges. This could explain the drop in N_1/N_2. The appreciably greater drop in BA/N_2 would be consistent with our earlier observations of the higher pumping speed of BA. It appears, in any case, that BA is more affected than N_1 by transient effects.

Because it is felt that some of our results are not sufficiently clear-cut, an improved version of the experimental arrangement is being set up, and further measurements will be made. However, even at this time there are some rather definite conclusions to be drawn: (a) the gauges are probably more reliable and less critical as to type (BA or N) and location in a clean system; (b) the Nottingham gauge is less affected by its location and general environment (e.g., presence or absence of oil vapors) than the Bayard-Alpert; and (c) when a large vacuum chamber is used, the gauge will provide a more accurate indication of pressure if it is mounted in the chamber than if it is off to the side in its own enclosure. The last conclusion was reached by Blears[3] some years ago; the present work leads one to ask whether the discrepancies would be nearly as large as those that he reported if one had a clean system, i.e., one free of oil vapors. Blears worked with a system in which the major gas component was oil vapor. Although he was aware of this fact, it is not clear whether he has concluded that his results would or would not have been different in a system containing permanent gases.

An all-metal vacuum system consisting of a mechanical pump followed by two cryogenic pumps and an ion pump has been assembled. A trap containing activated alumina will serve to trap pump oil vapors. It is hoped that, by pumping with each of the pumps, the mechanical and the two cryogenic, in sequence, the pressure can be reduced to a low value before the ion pump is started. This procedure should keep the ion pump relatively clean, and render much less serious its tendency to regurgitate previously pumped gases. It is hoped that this system will be a cleaner one than that presently used for routine evacuation of the tubes needed by this group. If tests show the new cryogenic system to be as good as we hope it will be, we will not carry through the work on evaluation of mercury diffusion pumps and various traps proposed earlier.[1]

A demountable vacuum chamber is being built that will allow us to make a variety of tests on such things as cathode emission and gas evolution. Provision will be made for continuous monitoring of gas composition.

Twelve diodes of a special design for laboratory evaluation of cathodes have been received from Sperry. Six of them were completely processed by Sperry; the others have been processed to the point of converting the cathode. We plan to do our own conversion on these, after which the tubes will be tested for emission under various pulsed conditions and then put on life test.

F. T. Worrell

VIII. SECONDARY EMISSION

The study of surfaces that have low secondary emission ratios and that are suitable for use in high-power microwave tubes has been completed. A report on this study is nearly finished. The three final tests described in this report were made on six plasma-torch coatings that in previous measurements had maximum secondary emission ratios less than unity. These tests were made in order to measure the effects upon the secondary emission ratio (δ) of these coatings by: (1) hydrogen-firing, (2) operation in a magnetic field, and (3) increasing the angle of incidence of the primary electrons.

The changes that occurred in the surface composition of several coatings during dry hydrogen-firing by outside vendors were not duplicated by our own firing of the pure powders. Therefore, it seemed worthwhile to respray all the coatings that in previous measurements had a $\delta < 1$. The coatings were sprayed in normal atmosphere; X-ray diffraction analyses of the sprayed materials were made, and the targets were then installed in a secondary emission tube. After measurements of δ, they were removed, fired in our own hydrogen furnace, again analyzed by X-ray diffraction, and installed in a second tube.

The effect of hydrogen firing and electron bombardment on δ is shown in Figs. VIII-1 through VIII-7. The data for WC and CrB_2 plotted in Figs. VIII-1 and VIII-2 show an increase in secondary emission ratio after hydrogen firing. X-ray diffraction analysis indicated that both materials were converted to metastable compounds (W_xC_y, Cr_xB_y) during the spray process, and that re-conversion to the original material occurred during hydrogen firing. Labeling the graphs as representative of WC and CrB is therefore not strictly correct.

Figures VIII-3 through VIII-6 are graphs of δ for VaB_2, TiB_2, TiC and CrC. None of these materials changed in composition when sprayed or hydrogen-fired. The slight decrease observed in δ after hydrogen firing is probably a result of surface cleaning caused by the firing process.

Figure VIII-7 is a comparative graph of δ for TiB_2, TiC, CrC, and VaB_2 after firing and electron bombardment. The hydrogen firing for all materials was at a temperature of 1025°C for 1 hour. Electron bombardment was at 10 kv with a power density of approximately 20 watts/cm^2 for 24 hours.

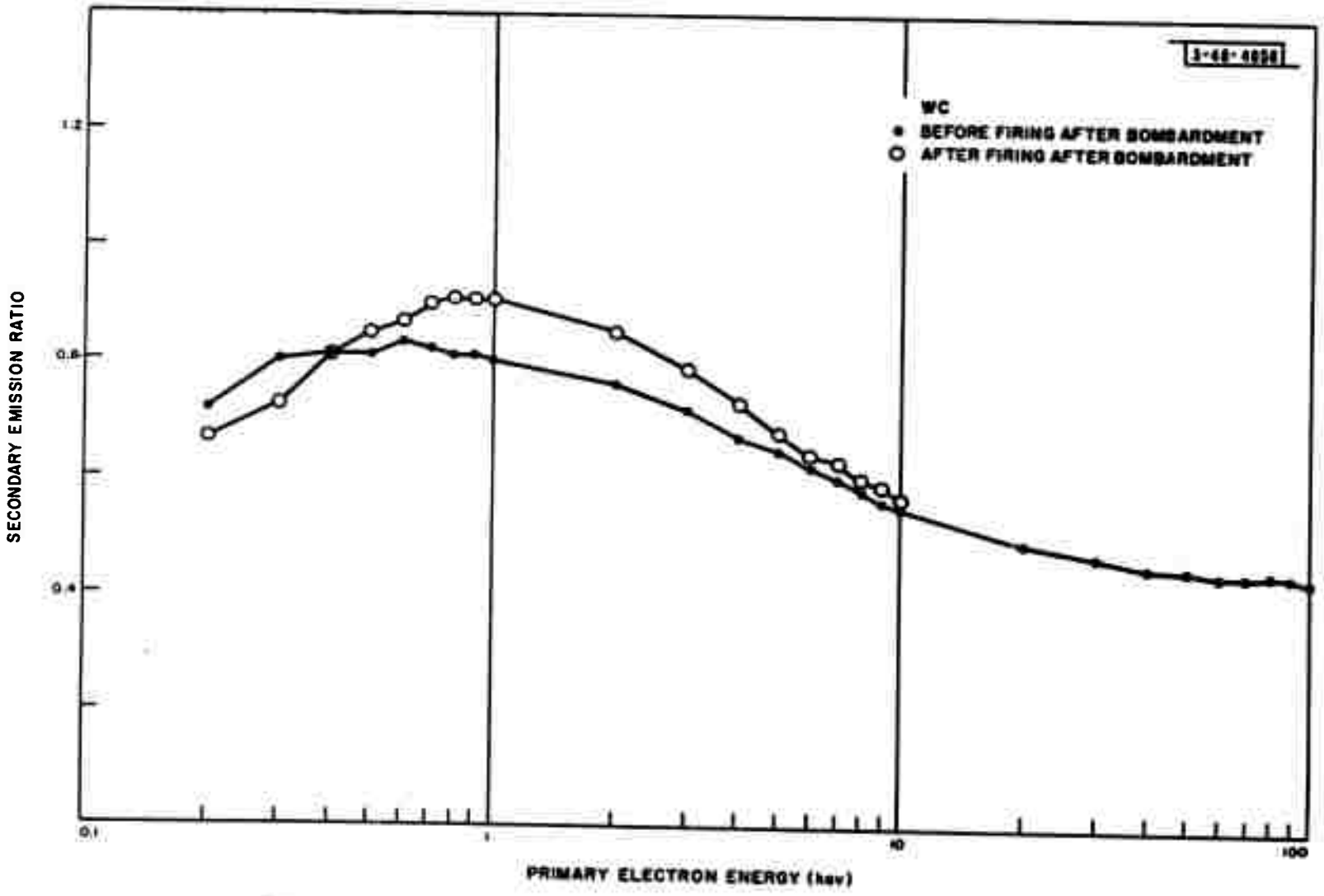

Fig. VIII-1. Secondary emission ratio of WC before and after firing.

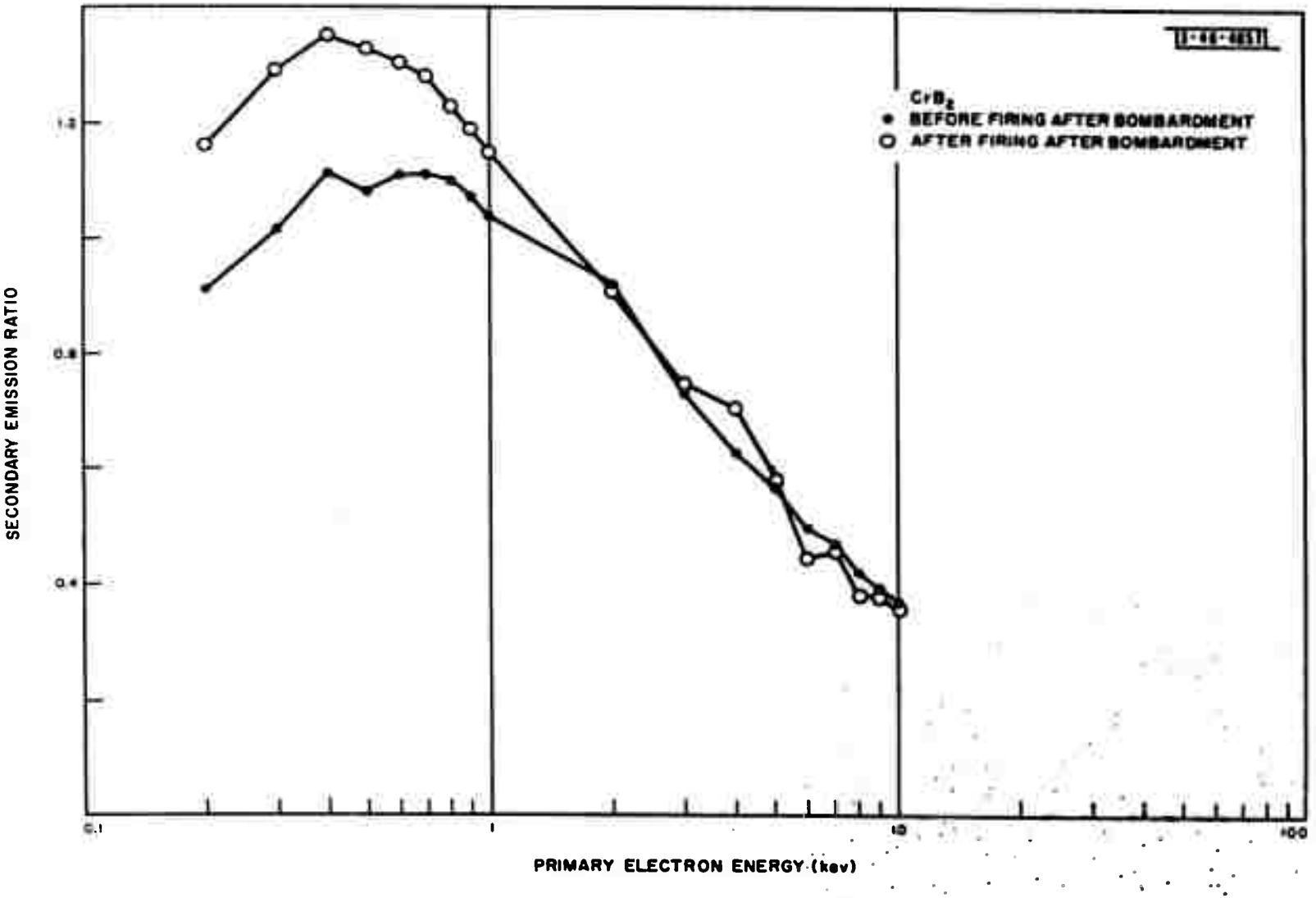

Fig. VIII-2. Secondary emission ratio of CrB_2 before and after firing.

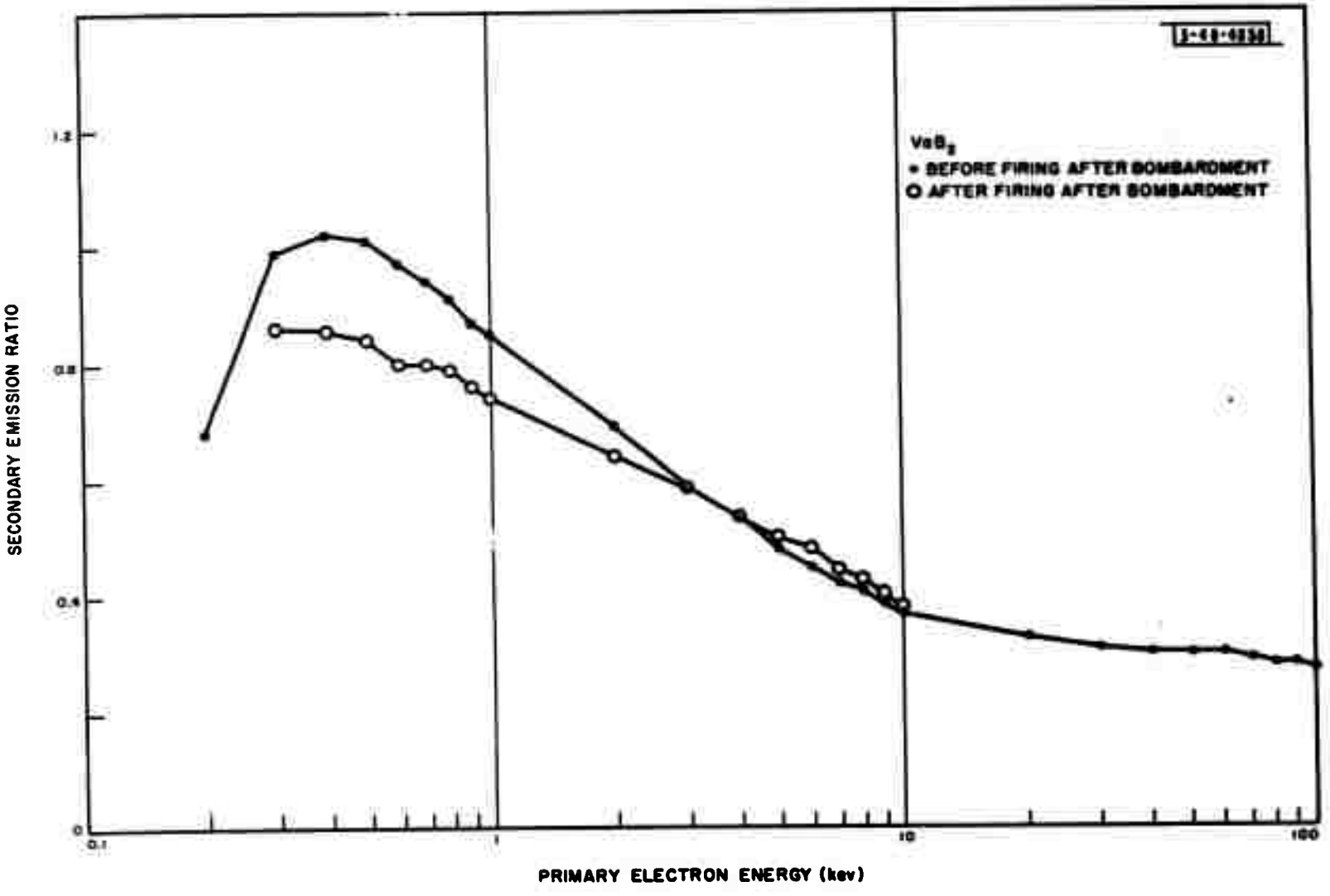

Fig. VIII-3. Secondary emission ratio of VaB_2 before and after firing.

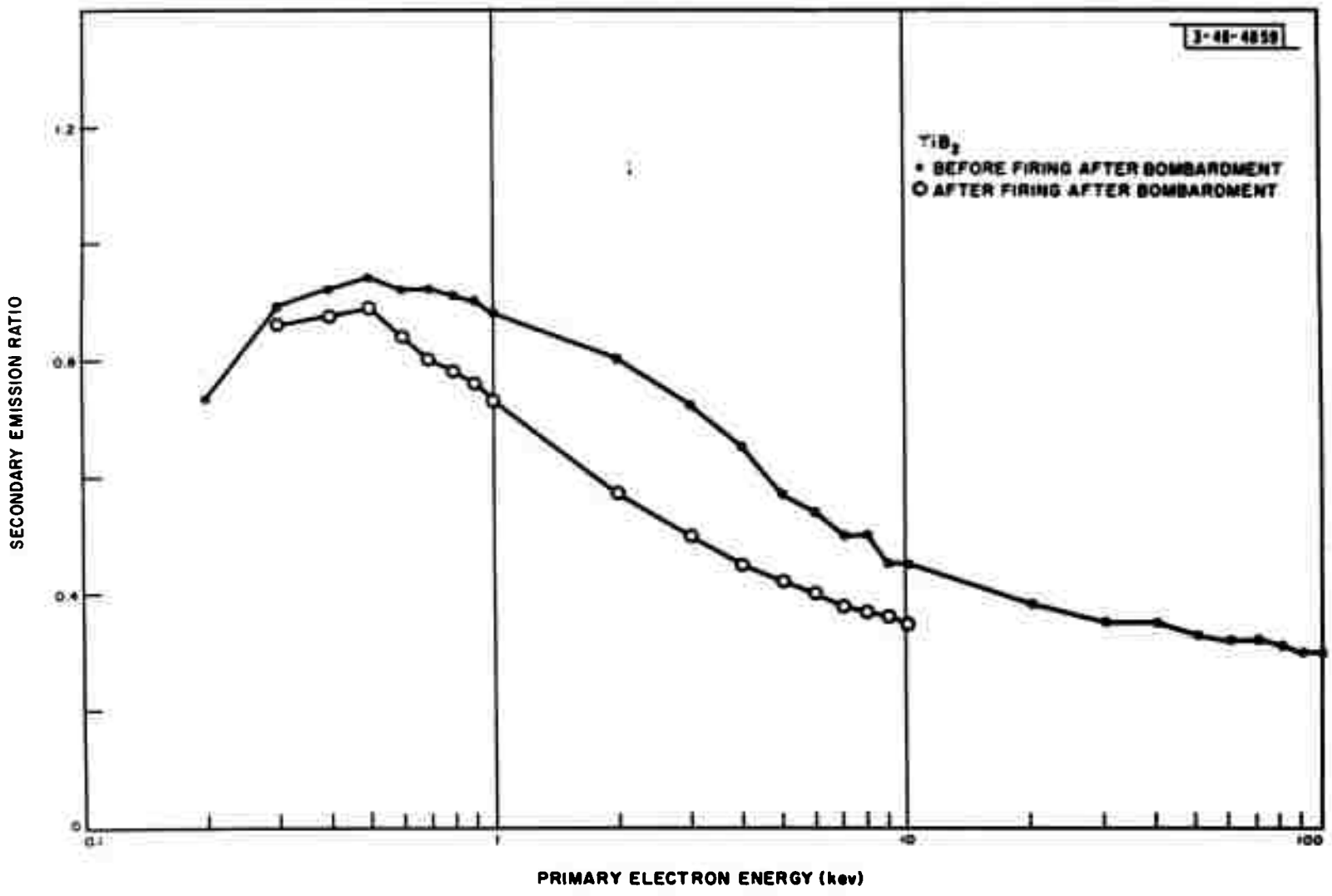

Fig. VIII-4. Secondary emission ratio of TiB_2 before and after firing.

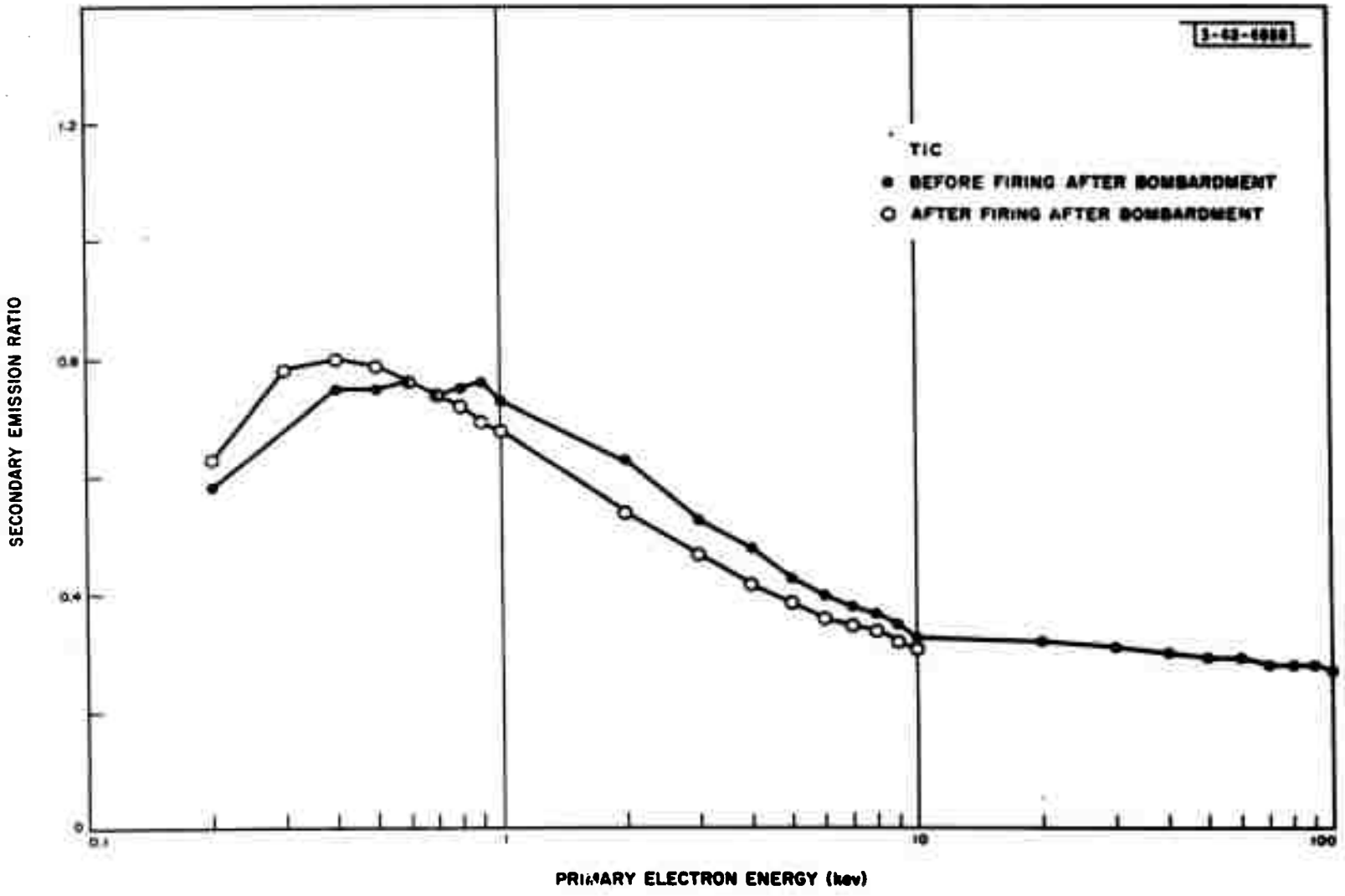

Fig. VIII-5. Secondary emission ratio of TiC before and after firing.

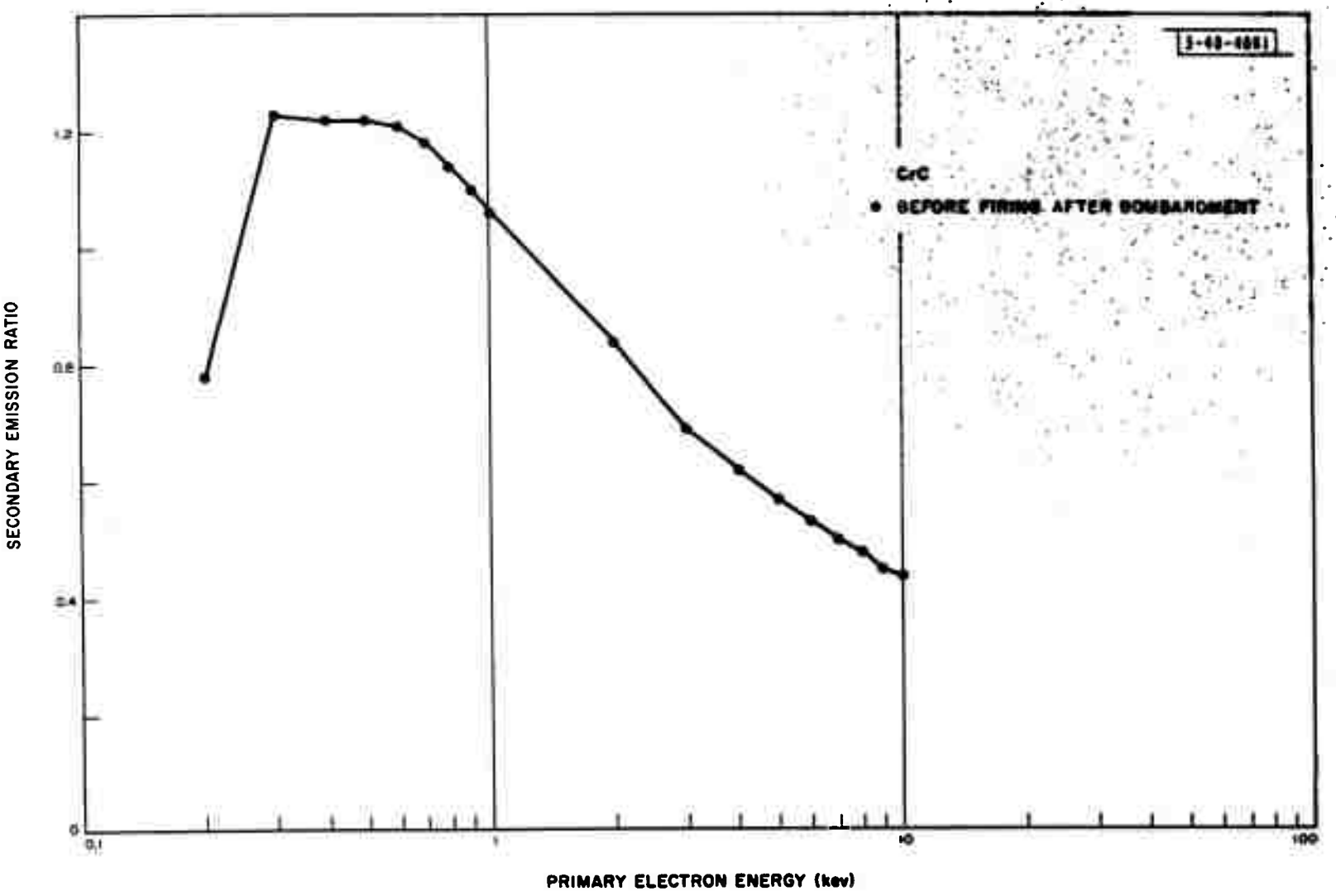

Fig. VIII-6. Secondary emission ratio of CrC before and after firing.

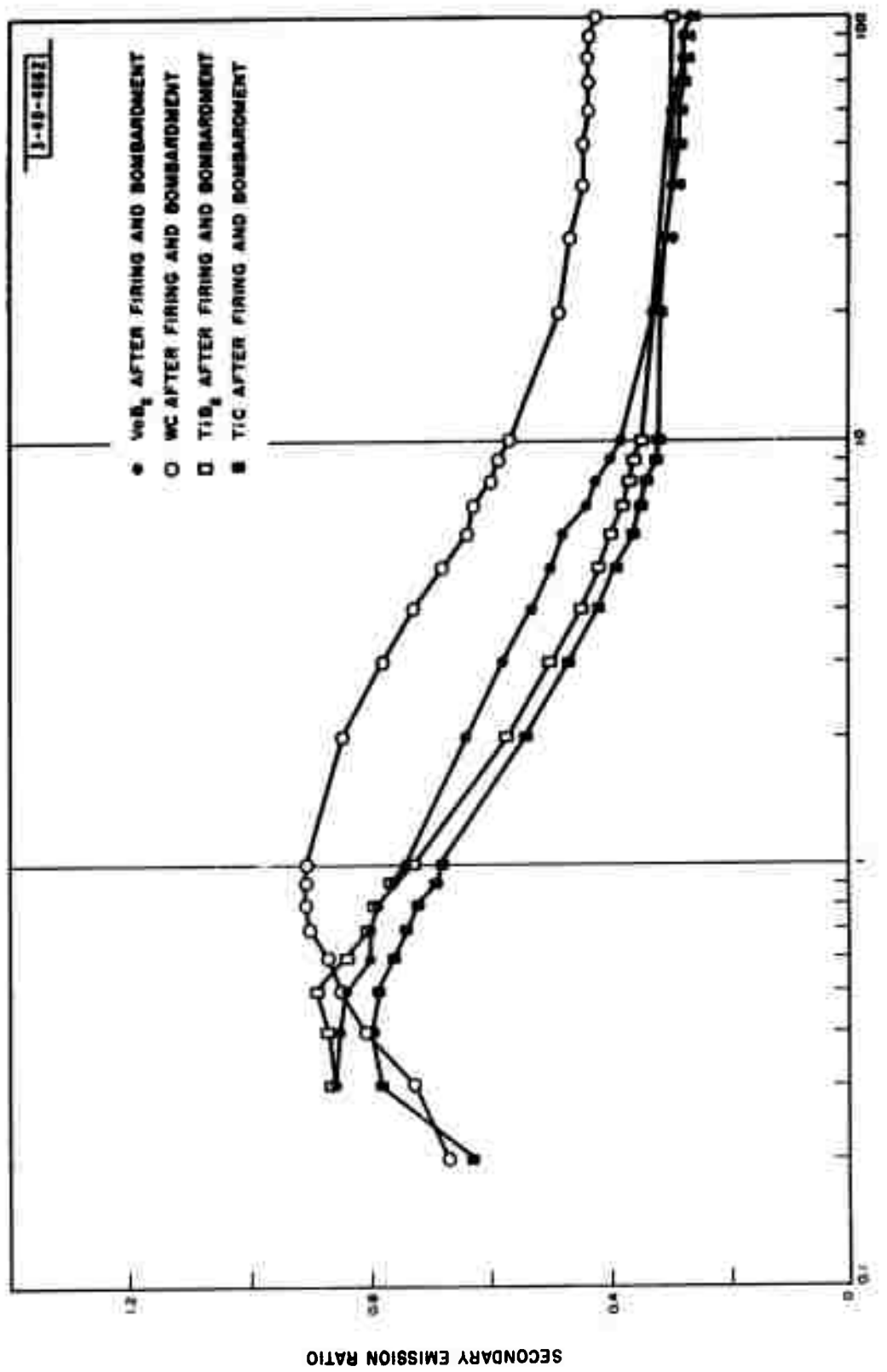

Fig. VIII-7. Secondary emission ratio of the materials with $\delta < 1$.

It had been reported to us that the δ of a rough or porous material increases in the presence of a magnetic field that is normal to the target surface. The effect is presumed to result from the fact that the secondaries are forced to travel along magnetic field lines that would lead them back along the path of the incident primaries and out of any valley or hole that might trap them. A 500-turn coil was wound onto the tube containing the six hydrogen-fired pebbly-surfaced plasma-torch coatings; this arrangement is shown schematically in Fig. VIII-8. The field normal to the center of the target is about 500 gauss and is approximately equal to that encountered in output gap circuits of some klystrons. Since coil heating was rapid, the field was turned on only for short periods while the target and collector currents were measured. The results of the measurements are plotted in Fig. VIII-9 for a primary electron energy of 1000 ev. At other primary energies the effect was similar. Note that the decrease in δ when the collector voltage Vc is at +10 volts and the field is 500 gauss can be nearly eliminated when Vc is raised to +80 volts. This effect is probably a result of secondaries leaving the surface obliquely and being turned back into the target's surface when there is only a small accelerating electric field produced by collector voltage. In any case, δ could not be increased in this experimental arrangement, so the effect of the magnetic field upon the δ of these coatings was not unfavorable.

There are published data[4] which indicate that the δ of many materials increases as the angle of incidence of the primary electrons is increased. The data on smooth copper indicate that δ can double as the angle of incidence (Θ) of the primary electron beam goes from 0 to 70°. One must assume, then, that in the case of rough surfaces where Θ is rather undefined, the δ, when Θ is 0°, must be higher than that of the smooth material. This point was verified in our earlier measurements of the δ of sandblasted copper surfaces.[5] So that the effect of Θ upon δ could be measured, the last tube constructed contained four targets on which there were one smooth copper surface, one sandblasted copper surface and four plasma-torch coatings. One target at a time could be suspended in such a manner that the target surface remained horizontal while the tube was tipped to the left or to the right as shown in Fig. VIII-10.

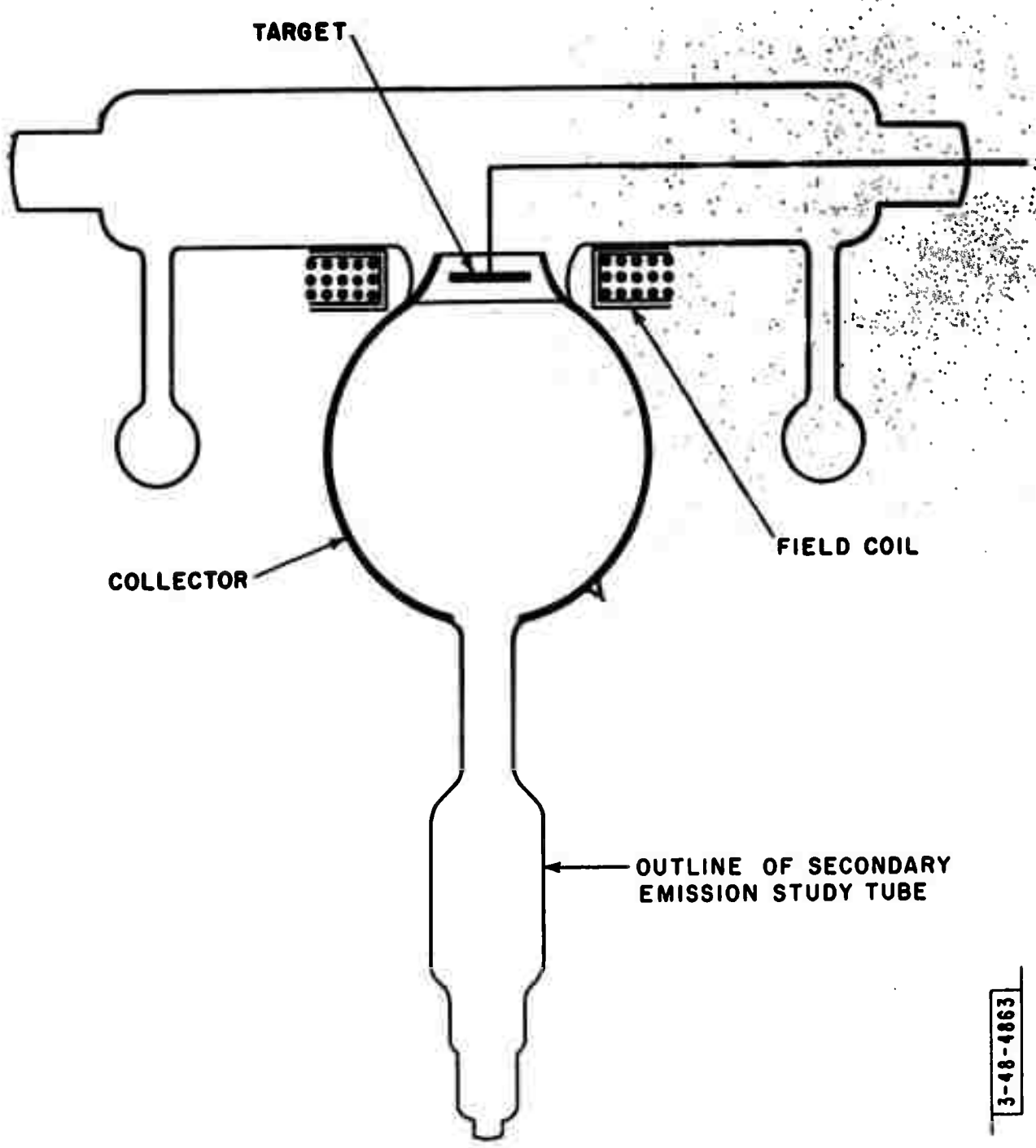

Fig. VIII-8. Outline of tube showing the location of coil supplying the magnetic field.

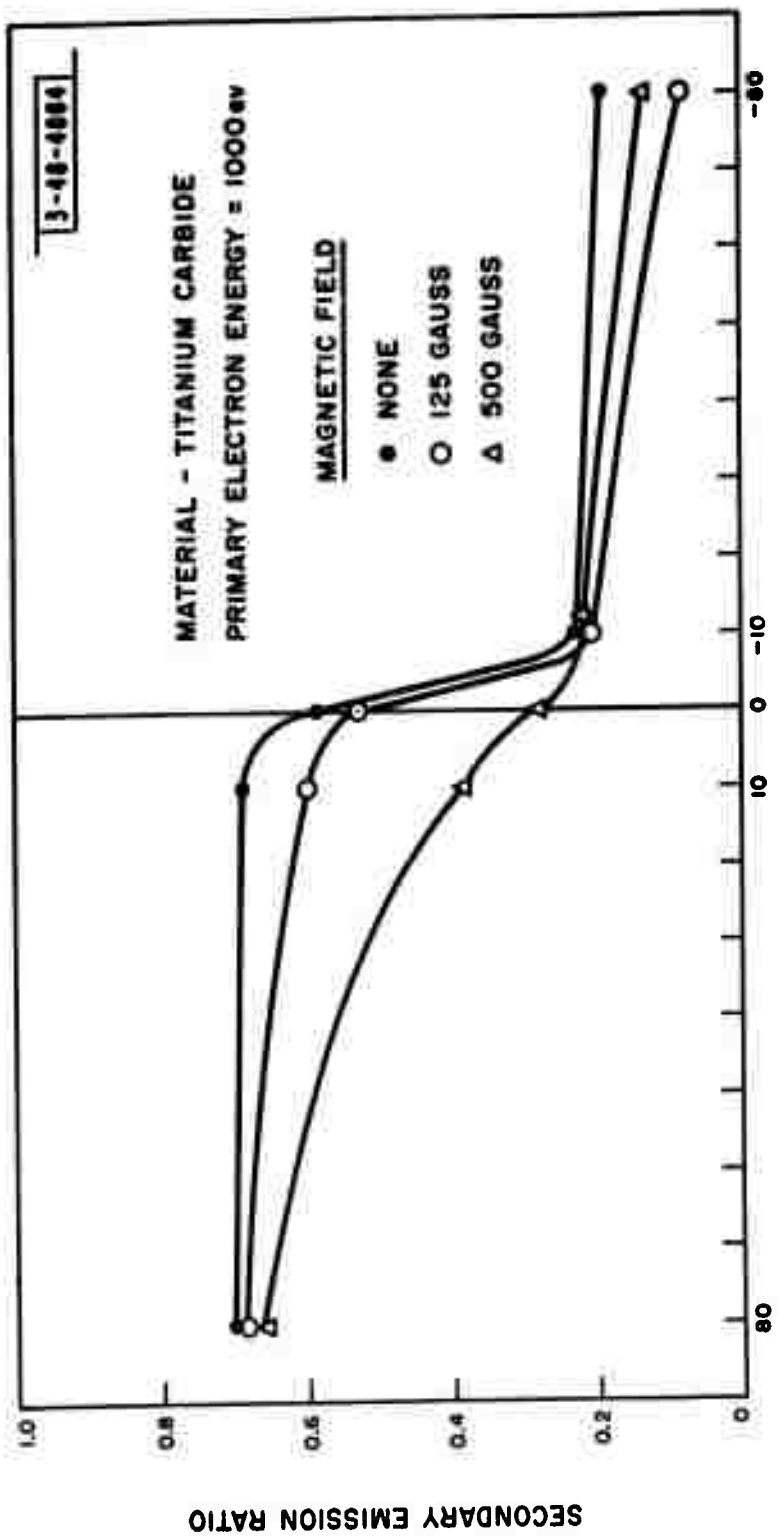

Fig. VIII-9. Secondary emission ratio vs collector voltage for three field strengths.

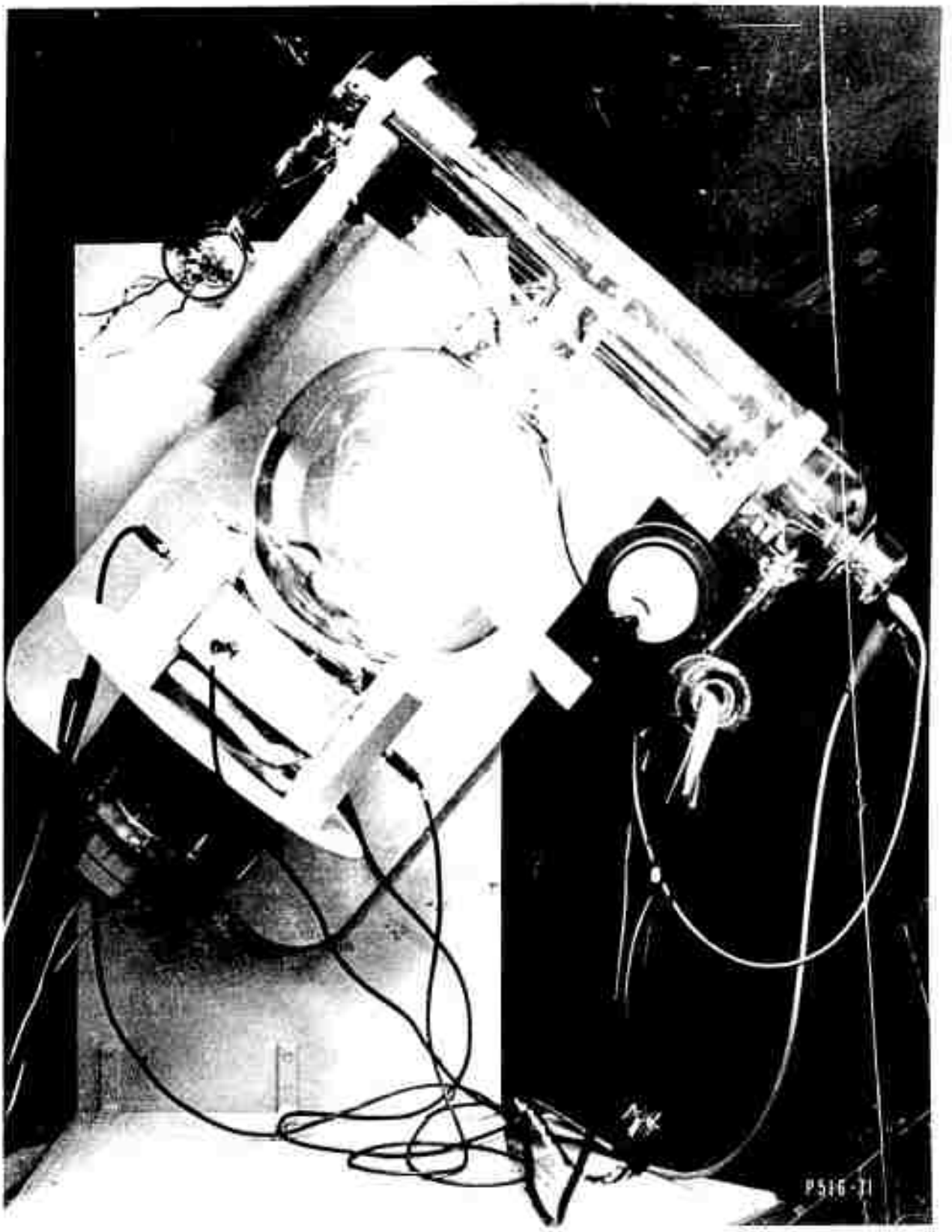

Fig. VIII-10. Secondary emission tube on tilting setup.

The δ's for three of these targets vs primary electron energy while Θ is at 0°, 40° and 60° are shown in Fig. VIII-11. The results for the two copper surfaces agree closely with published data. However, the very slight increase in the secondary emission ratio of the Titanium carbide with Θ, which is representative of the others tested, was a pleasant surprise. The measured δ for the smooth copper surface is 1.7 times that of the TiC when $\Theta = 0°$ and 2.5 times that of the TiC when $\Theta = 60°$.

In addition to completing the final report, there is a small amount of work yet to be done with the coatings in order to measure their DC and RF resistivities. There is some disagreement between RF measurements reported earlier,[1] data comparing RF resistivities of coatings and copper as calculated by cavity losses (see Section IX of this report), and the DC resistivities given in handbooks. Present plans are to coat a nonconducting material with these plasma-torch coatings, then measure the DC resistivities by conventional methods and RF resistivities by the cavity-loss technique.

A. Vierstra

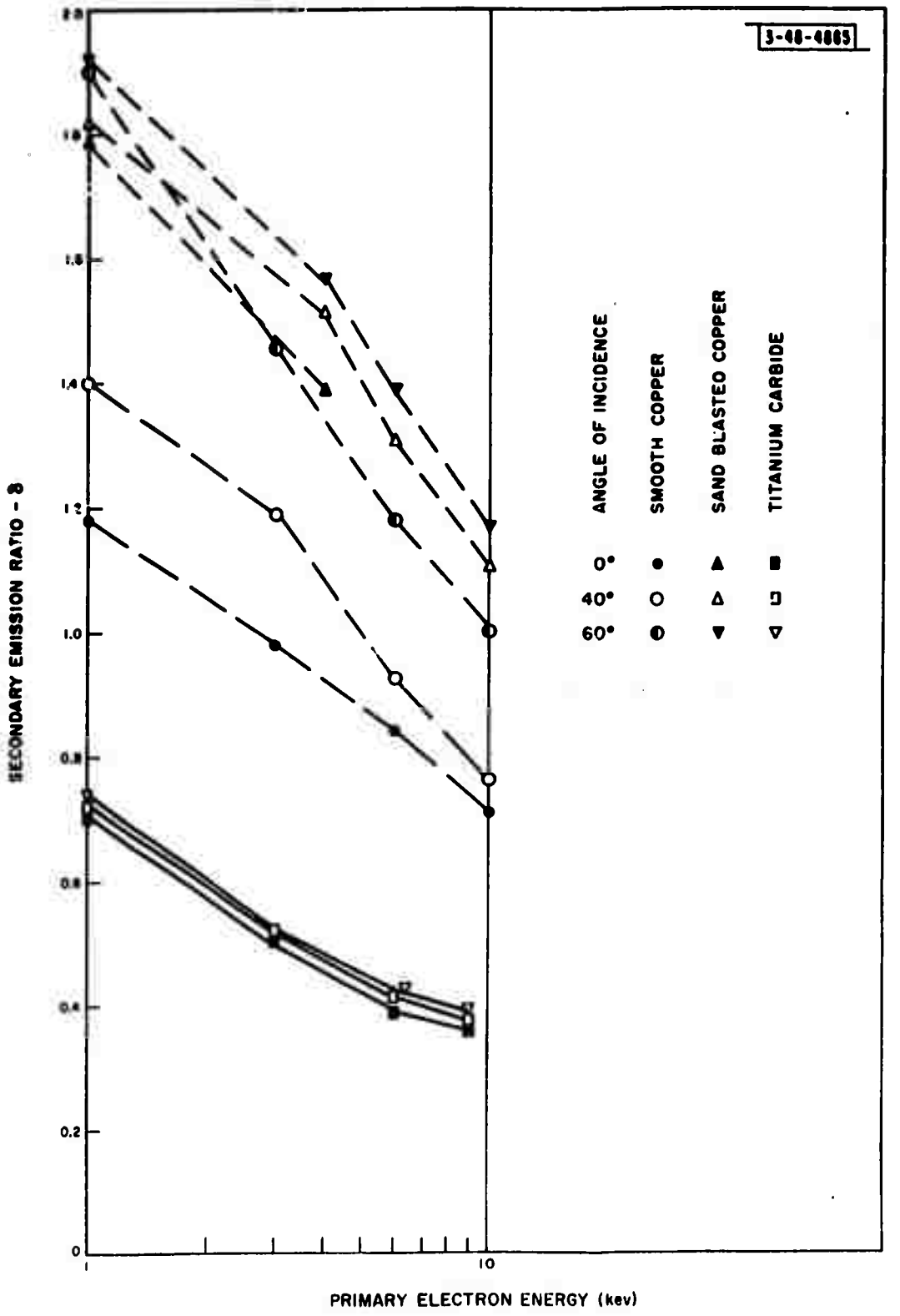

Fig. VIII-11. Secondary emission ratio of copper and TC at three angles of incidence.

IX. MEASUREMENTS OF SURFACE CURRENTS IN KLYSTRON CAVITIES BY THE PERTURBATION OF RADIATION FIELD

A new method for measuring surface-current distribution in microwave structures has been developed. This method, which is based on the perturbation of the field that radiates into the walls of the resonator, is simple as well as accurate and most suitable for this work. The perturbation equation for the Q of a resonator with n walls of different resistivities has already been derived:[1]

$$Q_u = \frac{2\int_V H^2 \, dv}{\sum_n \delta_r \int_{S_r} H^2 \, ds_r} \quad ; \tag{1}$$

where

Q_u = unloaded Q of the resonator,

H = magnetic field,

δ_r = skin depth of r^{th} wall,

S_r = r^{th} surface,

V = volume of resonator.

In deriving Eq. (1), the main assumption made was that the change in the over-all geometrical configuration of the mode field due to the perturbation of the radiation field is small. This would be true if the resistivity of each of the walls is changed by the same amount. (In this case the error in the numerator of Eq. (1) would be equal to $1/Q_u^2$, i.e., for a Q of 10, the error is 1 per cent.) For composite wall resonators, Eq. (1) is valid if the path of the surface current is little affected by the change of the wall resistivity. Throughout the course of our measurements, the Q was always high (above 1000) and the condition with regard to the path of the surface currents was always fulfilled; therefore, Eq. (1) is applicable.

The relative RF resistivities of the resonator walls were determined experimentally, since the RF resistivity depends to a great extent on the surface conditions as well as on the DC resistivity. Two identical reentrant cavities,

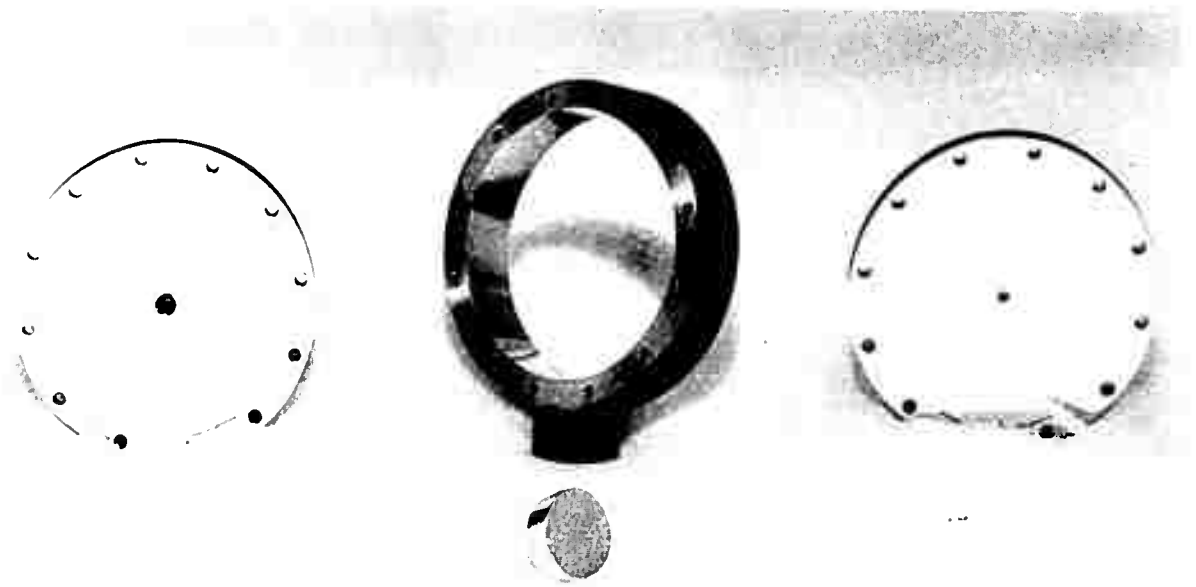

Fig. IX-1. Reentrant resonator (under test) constructed of four walls.

one brass and the other copper, were constructed, each being made of four similar walls (Fig. IX-1). The unloaded Q's of the two cavities were measured. The results were 7950 for the copper cavity and 4000 for the brass cavity. Thus, the effective skin depth for brass is 1.97 times that of copper.

The procedure for measuring the surface current in each of the four walls of the cavity was to interchange the brass and copper walls to form composite brass-copper cavities and measure their unloaded Q's. In order to check the results, measurements were taken on two sets of four composite cavities. The first set was made up of three walls of copper and one of brass, while the other set had one copper wall and three brass walls. The average of the results of the two sets is shown in Fig. IX-2. The average of the sums of the percentage losses on the four walls is 100.5 per cent, which is the average of 101.5 per cent for the first set and 99.5 per cent for the second set. Particular attention was given to wall No. 4 of Fig. IX-1 in order to find the field distribution on the drift tube wall. By spraying annular rings of materials of known resistivity and certain width (about 0.050 in.) at different positions on wall No. 4 (Fig. IX-3), and measuring the change in Q, it was possible to calculate the relative field strength along the surface. Since the spraying was not uniform, the plotted curve of the relative field strength was not completely defined. However, the results indicated that about one-third of the 15.3 per cent (the total loss on wall No. 4) is on the half near the gap edge, and that two-thirds are in the other half. A new method that employs copper plating on stainless steel to form annular rings has been developed and further measurements are being taken. It is expected that, by this method, more accurate results for the field distribution will be obtained.

Once the field distribution on the walls of the cavity had been determined, it was then possible to measure the RF resistivity of some of the materials that have low secondary emission ratios; namely, VaB, WC, TiB, TiC, CrB and CrC. The measured RF resistivities of these materials are listed in Table IX-1. The observed values are one to two orders of magnitude greater than the DC values reported in the literature. The reason for this large difference is not known. Tests on sprayed copper coatings make it appear that the roughness of the surface is not the primary cause of the high resistivity

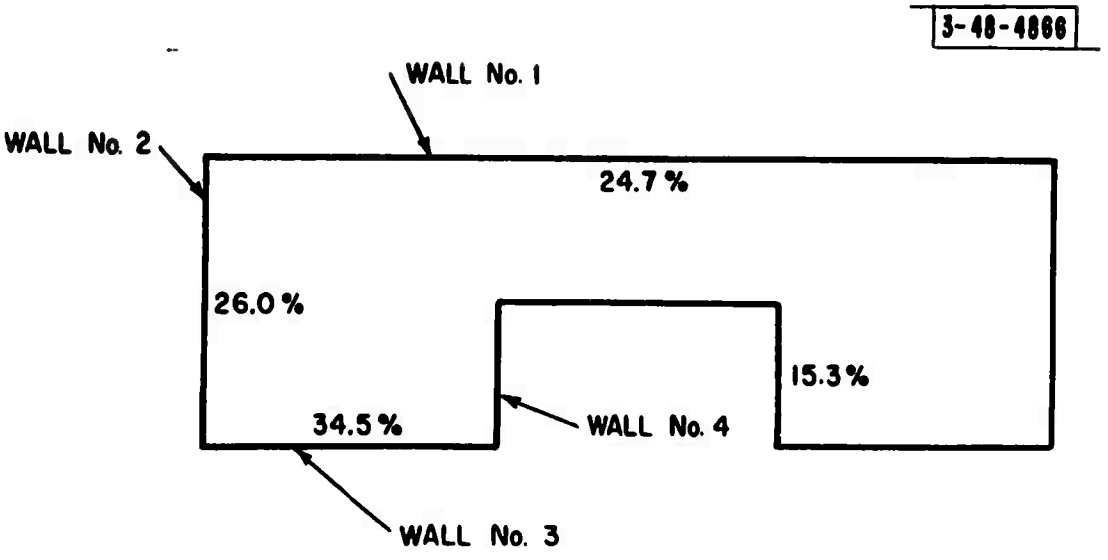

Fig. IX-2. Average surface current on the four walls of a reentrant resonator.

P516-64

Fig. IX-3. Drift-tube wall with resistive annular rings shown at different positions.

TABLE IX-1

RF RESISTIVITY AT 3 kMcps

Material of Wall No.4*	Q_u	Skin Depth Relative to Copper	Resistivity at 3 kMcps Relative to Copper	Reported DC Resistivity
Copper†	7950	1	1	1
Brass†	6965	1.97	3.90	3.9
S.S.†	4270	6.7	45	42.5
VaB‡	4140	6.9	48	16
WC‡	2590	14.6	214	12 – 53
CrB‡	2230	17.9	320	21
CrC‡	2220	18.0	325	–
TiB‡	1770	24.0	577	15 – 30
TiC‡	1700	25.2	636	68

*The other three walls are copper.

†Mechanical polish.

‡Plasma-torch spraying.

(no significant change in resistivity of a sprayed copper surface occurred when the surface was ground to a smooth finish). To investigate the factors affecting the RF resistivity of plasma-torch coatings would require further experimental work. Such an investigation would be beyond the scope of this project, which will be concluded in the next few weeks. A comprehensive report is now under preparation as a group report.

The main factor limiting the accuracy of this method of measuring surface current is the precision with which the Q can be measured. Two methods for measuring the Q were considered. The first is that of measuring the difference in phase between the detected modulation of an AM signal before it passes through the resonator that is tuned to the carrier frequency,[1] and after. The

second is the conventional method of determining the half-power bandwidth of the amplitude-frequency response. The second method was found to be superior to the first for values of Q in the range below about 10,000 because a suitable wide-band high-frequency phase meter was not available. A block diagram of the setup for the second method, which was used in all the experimental work, is shown in Fig. IX-4.

M. Nader
I. Hefni

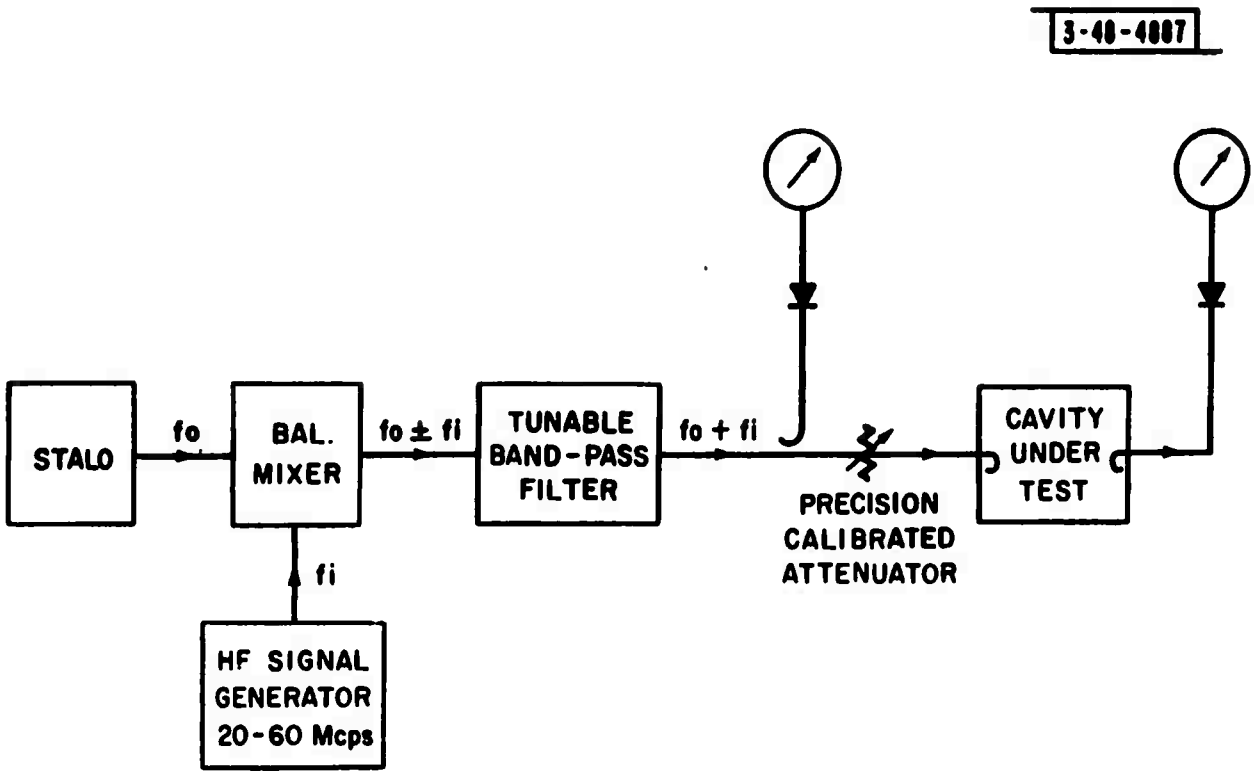

Fig. IX-4. Simplified block diagram for measuring the Q of resonators.

X. LIMITATIONS ON THE BANDWIDTH OF KLYSTRON OUTPUT CAVITY

The bandwidth of klystron amplifiers at high signal levels is rather difficult to define because of the nonlinearity in the gain vs signal-level characteristic. Several definitions[6] of large signal bandwidth have been suggested that would be useful for practical purposes. Such definitions, however, cannot be formulated rigorously in terms of the tube parameters since the exact behavior of the beam at large signals is not yet known. For this reason it is not possible to obtain the theoretical limitations on the bandwidth by considering all the tube parameters, and most of the work on optimizing the bandwidth has been done on a step-by-step basis. At the present time, the factor that is limiting the bandwidth of the multicavity klystron seems to be the output coupling to the load. Several attempts[6,7,8] have been made to optimize the output coupling by using passive matching structures. It is rather difficult to estimate the degree of success of these attempts, since the results were not compared with the correct theoretical optimum. The purpose of this work, therefore, is (1) to investigate the theoretical limitations on the bandwidth of an idealized output coupling that can approximate an actual coupling at small signal operation, and (2) to develop an optimum matching structure which would be suitable for high-power operation.

Assuming a linear beam-circuit coupling, the limiting factor on bandwidth for a conventional output gap would be the gap capacitance C, shunted by the beam conductance G. The theoretical limitation on the bandwidth for such a simple equivalent circuit was first derived by Bode[9] in the form of the integral relation

$$\int_0^\infty \ln \frac{1}{|\rho|}\, d\omega \leq \pi \frac{G}{C} \quad , \tag{1}$$

where $|\rho|$ is the magnitude of the reflection coefficient as shown in Fig. X-1. The inequality sign in Eq. (1) occurs in the degenerate case when the matching structure starts with a capacitance. Such a degenerate case cannot

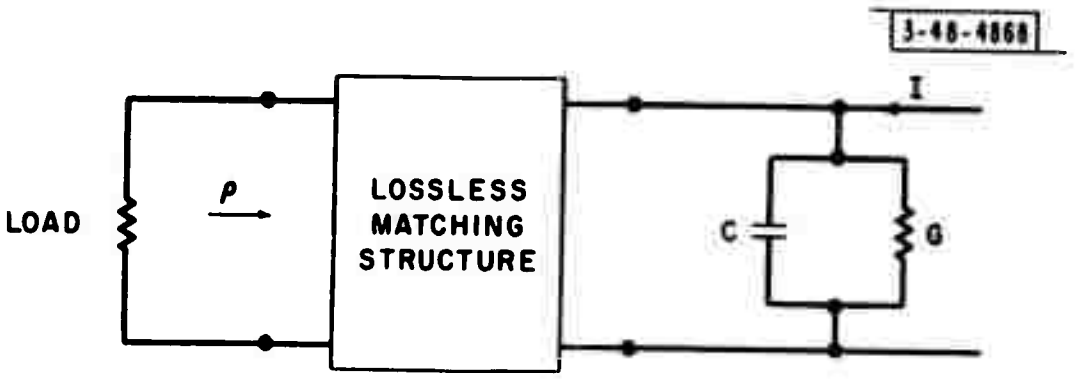

Fig. X-1. Equivalent circuit for the output load coupling of klystron amplifier.

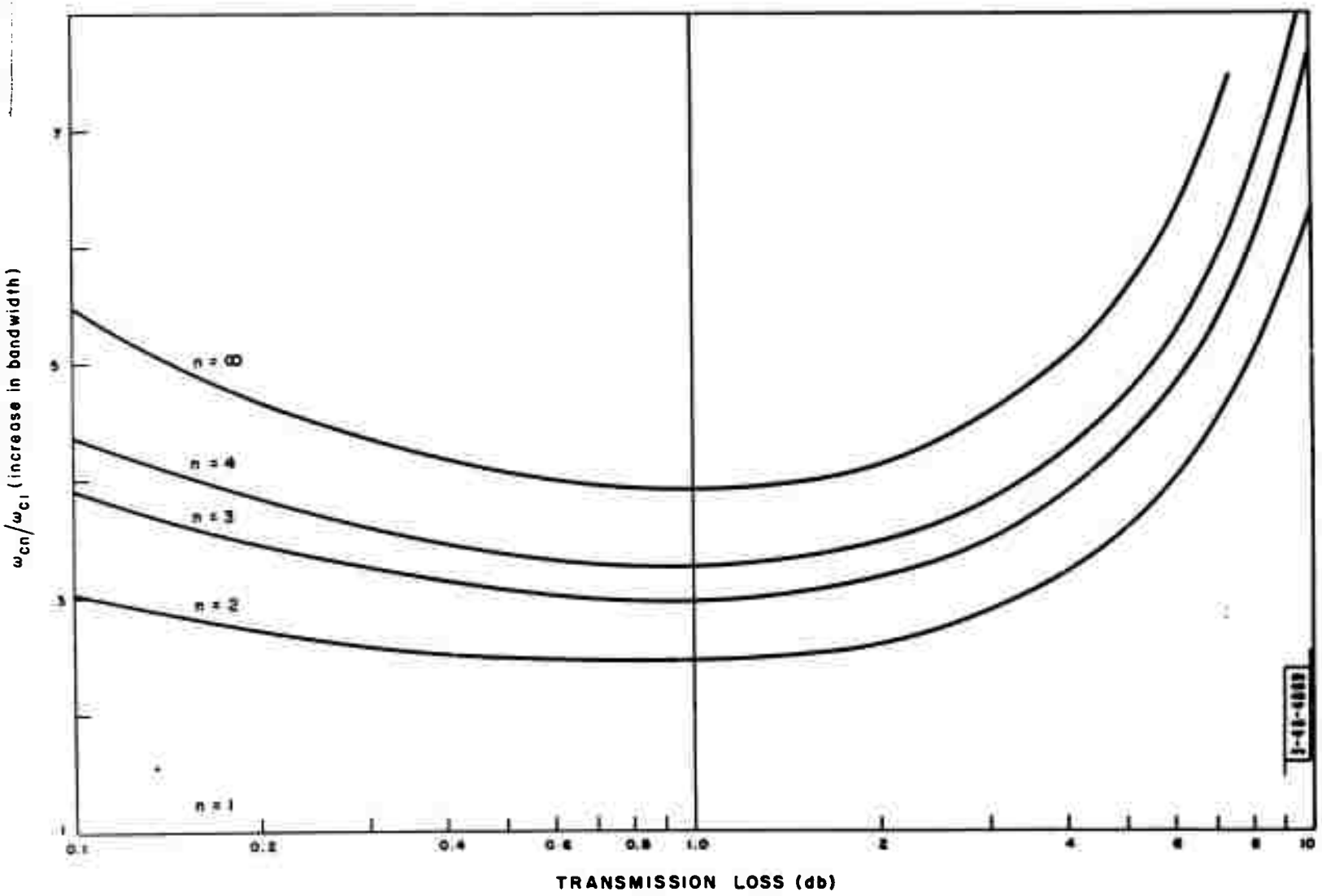

Fig. X-2. The theoretical increase in bandwidth when matching networks with one, two, three and infinite (n = 2,3,4 and ∞ respectively) numbers of elements are used.

be avoided at microwave frequencies, since, when the gap is incorporated in a resonator, part of the electric field will be stored outside the gap capacitance, resulting in an increase in the effective coupling capacitance. The first step for optimizing the bandwidth would, therefore, be to design a resonator with maximum concentration of the electric field in the gap capacitance. This must be done empirically, since an exact solution is impossible. Having optimized the resonator, one may assume a new equivalent shunt capacitance, and the analysis for optimizing the bandwidth can then be carried out rigorously.

Equation (1) shows that the optimum bandwidth would be achieved when $|\rho|$ is kept constant over the pass band and equal to unity over the rest of the frequency spectrum. In this case Eq. (1) reduces to

$$\ln \frac{1}{|\rho|_{max}} \cdot \omega_c = \prod \frac{G}{C} \quad ,$$

where ω_c is the cut-off frequency for a certain mismatch $|\rho|_{max}$. This rectangular shaped function cannot be realized in practice, since it would require a matching network with an infinite number of elements. A good approximation for the rectangular function would be a Tchebyscheff function with the ripple amplitude chosen to minimize the transmission loss over the desired bandwidth. The analysis for this optimization results in two transcendental equations that can be solved numerically. The solution has been computed for matching networks with different numbers of elements at different values of mismatch. Some of the results are plotted in Fig. X-2, which shows the increase in the bandwidth ω_{cn}/ω_{c1} one should expect when matching networks of one, two, three or infinite ($n = 2, 3, 4$ or ∞ respectively) numbers of elements are used.

An experimental verification of this theory is planned.

I. Hefni

XI. VOLTAGE BREAKDOWN

This project was established to investigate the possibility of devising techniques that would permit the safe use of higher voltage gradients in microwave tubes where voltage breakdown is frequently a limiting factor in power output. The major portion of the experimental work has been directed toward achieving a high voltage hold-off capability for pairs of nickel or copper electrodes. The type of data that is recorded is shown in Fig. XI-1, where voltage pulses of 1 msec are applied to the gap at 5-second intervals and the number of breakdowns per group of ten pulses is plotted vs voltage. The conditioning process is very evident in this type of graph and on the 14th group of pulses the pair of electrodes used holds off 65 kv with no breakdowns, although the initial breakdown point was 35 kv.

Data recorded in the same manner for copper electrodes with various surface treatments is as follows:

	Initial breakdown voltage	90 per cent breakdown point while increasing voltage	Final hold-off voltage
Surface sandpapered with a ++600	10 kv	30 kv	35 kv
Mechanically polished	45	60	70
Electro-polished and "glow cleaned"	60	70	80

The "glow cleaning" is accomplished by a 200- to 300-volt AC discharge in a low-pressure hydrogen atmosphere. The direct voltage hold-off capability (no breakdowns in one minute) on these electrodes is only 10 per cent less than the 1-msec pulse voltage hold-off, which appears to indicate that this 1 msec pulse is long enough to be close to the DC hold-off voltage.

Some measurements made on plasma-torch coatings such as one used in the secondary emission study indicate that they hold off about the same voltage as polished copper. More measurements will be made on these plasma-torch coatings and on other materials that the literature suggests have a higher voltage hold-off capability than copper.

A. Vierstra

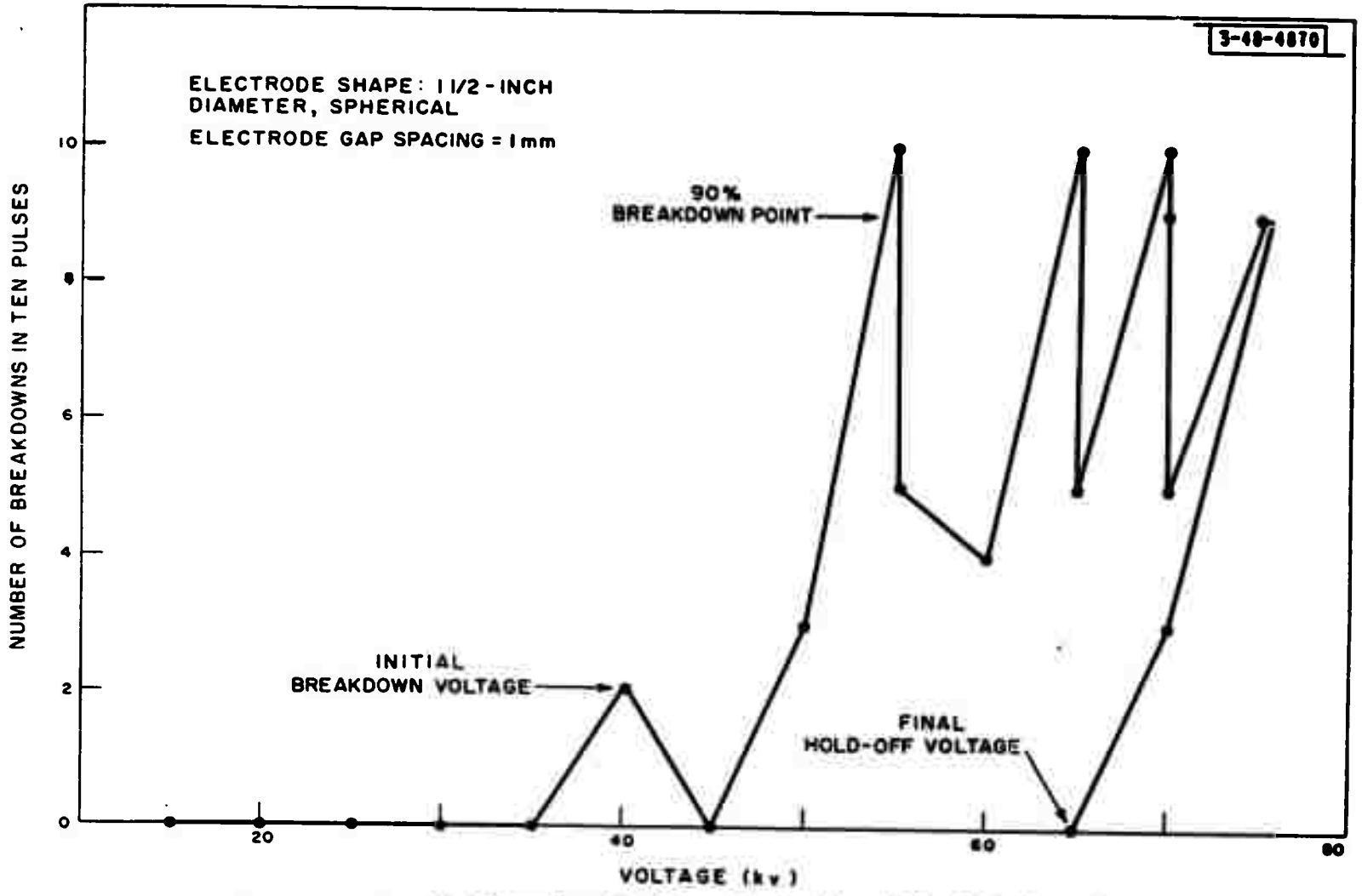

Fig. XI-1. Results of experiment with mechanically polished Ni electrodes.

XII. DUPLEXER INVESTIGATIONS

A. PAPER PRESENTED AT PGMTT

A paper entitled "High Power Duplexers" was presented at the IRE 1961 National Microwave Symposium (Washington, D.C., 15-17 May). An abstract of this paper and of Lincoln Laboratory G-Report 46G-0011 follows:

> The various circuit arrangements used in duplexers are analyzed as to their power handling abilities in two situations: first, where the bandwidth is narrow so that insertion loss determines maximum Q and second, where large bandwidths are required and the maximum Q is determined by available Q bandwidth products. In both cases the ATR duplexer has an advantage. Arc loss was measured for folded cylinder TR tubes. At medium current densities the results agree well with experimental measurements in DC positive columns. At high current densities a constant conductivity is reached. Graphs of power handling ability for a unity coupler duplexer using different methods of cooling are presented. It is shown how the requirements for easy firing and long life limit the achievable recovery time.

The most interesting result presented in the paper is a graph of the power-handling capability of a full-size TR window mounted in the broad wall of a waveguide (Fig. XII-1). Adjacent to the window is a highly ionized gas. Results of calculations for different methods of cooling show that dielectrics with high heat conductivity, particularly beryllium oxide, are to be preferred as window material. With this in mind, vendors are being approached with the problem of fabricating a suitable window made of beryllium oxide for S-band use. It is of importance to note that in TR service the relatively high loss tangent of the BeO is of no consequence, since the heat is generated in the discharge and not in the window. This is quite different from the situation that exists in RF output windows, where the heat is generated by internal losses.

B. PIRANI GAUGE

In handling clean gases, it is essential to use a pressure gauge that will not contaminate the gas. This is especially true in sealed-off tubes where the gauge is exposed to the tube for long periods of time. A Pirani gauge seems

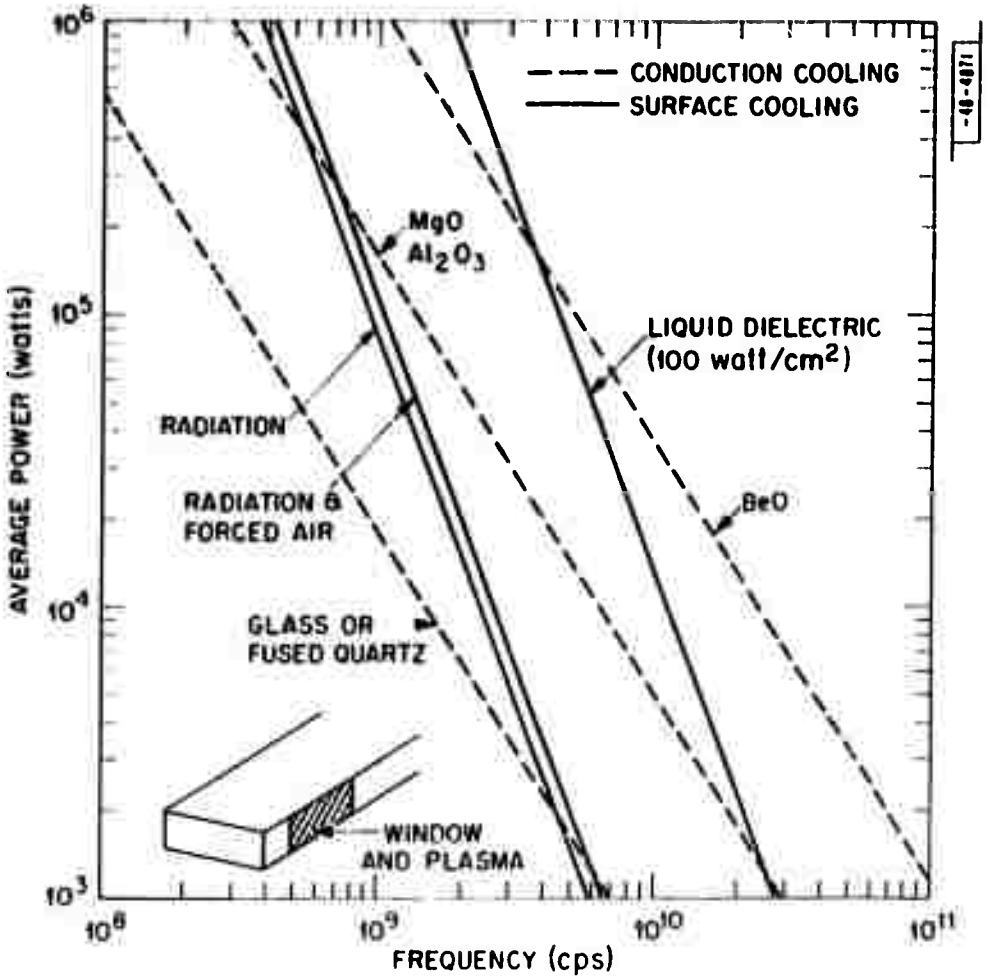

Fig. XII-1. Power-handling capacity of large waveguide window with high-density plasma.

admirably suited for measuring pressures in the micron and low millimeter range. It consists of a piece of wire located inside the pressure chamber. Several gauges, consisting of 0.001-in. diameter tungsten wire about 3-1/2 in. long mounted in the center of a 1-mm diameter capillary tube, were procured. The best mode of operation for these gauges is as the fourth arm of a bridge that is always maintained in a balanced state. The gauge always operates at a constant resistance and temperature. The heat loss from the gauge consists of two parts: (1) at zero pressure, heat is lost by conduction along the gauge wire to the mount and by radiation from its surface; and (2) as the pressure increases, heat is carried away by gas molecules that strike the wire and leave the gauge with more energy than that with which they arrived. This second heat loss is directly proportional to pressure at low pressures, and constant at high pressures. For a given gauge used with a particular gas, the above considerations lead to the calibration equation

$$P = P_o \frac{V^2 - V_1^2}{V_2^2 - V^2} ,$$

where V, V_1 and V_2 are the voltages across the bridge necessary to maintain balance at the pressure P, zero pressure and very high pressure, respectivel P_o is the pressure at which the second heat loss due to gas conduction changes over from a linear function of pressure to become independent of pressure.

To test the gauge, a self-balancing bridge was constructed and calibration curves were run on several gauges. The above equation was found to fit the calibration curve within experimental accuracy. The largest systematic error seems to be due to the change in ambient temperature between calibration and use. Examination of the sources of heat loss mentioned above indicates that the percentage change in V_1^2 should be between 2 and 3 times the percentage change in the ambient temperature measured in degrees Kelvin. This has bee confirmed by experiment. The change in ambient temperature thus limits the lowest pressure that can be read. A thermostatically controlled bath is being considered. The highest pressure that can be read with any accuracy is about $3P_o$. The present gauge can be used to read argon pressures from 5 microns

to 10 mm Hg. It is intended to use this gauge in all TR work where accurate control of gas fill is required.

C. HOT CATHODE TR

A gas TR used as a protector invariably requires some source of predischarge electrons to provide reliable breakdown and a low-energy spike. The classical solution to this problem is to use a keep-alive electrode that maintains a slight discharge in the region of the RF gap. The apparent simplicity of the keep-alive is belied by the host of problems it introduces. The discharge is inherently a high-voltage phenomenon. The large cathode fall produces high-energy positive ions that rapidly clean up the gas in the tube. Relaxation oscillations of the keep-alive current are difficult to avoid and can allow occasional high-energy spikes. The current drawn is inefficiently used since, typically, only a very small portion provides electrons in the RF gap. A radioactive source of electrons would seem to be a solution, but radioactive sources that would not require special precautions have not proved effective except for starting a keep-alive discharge, because radioactive sources typically supply very-high-energy electrons. A source which supplied a sufficient number of electrons would be too radioactive to handle safely.

The use of an electron gun to provide electrons presents the possibility of reliable breakdown and a low-energy spike without producing high-energy ions to clean up the gas in the tube. By placing the gun outside the RF gap and by keeping all electrode voltages below breakdown level, the effect of the gun on a low-level signal should be negligible, except for the introduction of some shot noise. If necessary, the gun current can easily be pulsed.

A few preliminary tests have been performed on a TR tube incorporating an electron gun as a source of predischarge electrons. The tube, TUCOR TX48UX2, has a parallel-plate gap with a hole in one plate for injection of electrons from the gun.

The effectiveness of the gun in reducing the breakdown voltage is best shown in single-pulse breakdown. With no gun current, firing took place in about 60 μsec with 810 volts of RF. This was the lowest level for which the breakdown time was reasonably constant. Occasionally, however, the tube would not fire

at this level. With about 2.5 μa of gun current through the gap, the breakdown level was reduced to 9.7 volts for consistent firing at 60 μsec. For comparison, the breakdown voltage of a BOMAC BL994 without keep-alive current was 705 volts. With 50 μa of keep-alive current, the breakdown voltage dropped to 23 volts. Increasing the keep-alive current to 150 μa did not further reduce the breakdown voltage.

The noise contribution of the TR tube was determined experimentally by measuring the noise figure of a receiver preceded by the TR tube in a high-Q cavity. The increase in noise figure with gun current can be considered an increase in the source temperature of the receiver. A calculation of this temperature based on the shot noise of the gun current through the gap agrees within about 20 per cent with the experimental value. With the gun current used for the breakdown measurements (approx. 2.5 μa), the temperature increase was about 40°K. The temperature is proportional to both the Q of the TR cavity and the gun current. Each of these could probably be reduced, or the gun current could be switched off for receiving in actual operation, in order to reduce the temperature contribution of the TR tube. The noise-temperature increase with the BL994 showed the same type of current dependence, but the keep-alive current for a 40° rise was about 140 μa, since only a fraction of this current passes through the electrode gap.

Because of the dimensions and fill of the TX48UX2, the recovery time was about 1500 μsec. A version presently being constructed using a helium fill and a shorter gap should have a recovery time on the order of 100 μsec. Life tests on this unit will be started in the near future. In this unit, since there should be no high-energy positive ions present, the gas cleanup should be slow and the tube life should be long. If life tests are satisfactory, it is expected that this type of tube will find use as a protective TR, where its low firing voltage will keep leakage energy to very low levels.

D. L-BAND INVESTIGATIONS

The design of an L-band duplexer cavity was mentioned in the previous semiannual report.[1] A quartz folded cylinder TR tube of 1.100-in. diameter was mounted horizontally in a capacitive iris across a rectangular cavity. Low-power tests showed that spring finger contacts onto the tube had a

detrimental effect on the unloaded Q of the cavity. A considerable improvement was obtained by making the tube a precision fit in a 1/2-in.-thick iris, giving an unloaded Q of 5500.

The cavity was side-wall mounted in a WR650 waveguide and high power tests were carried out using a traveling wave resonator. Using a 2-Mw peak and a 4-kw average power magnetron, resonator powers of 40-Mw peak could be obtained with an air pressure of 30 lb/in.^{2} in the ring. The duplexer cavity tested was not pressurized, but showed no evidence of sputtering at the highest peak power at which it was tested (10 Mw), with a value of Q_{L1} of 22.

The temperature of the TR tube was monitored at various values of average power (P_{av}), duty ratio (Du), and loaded Q (Q_{L1}); from the results, it appeared that the dissipation on the tube was proportional to the quantity

$$\sqrt{\frac{P_{av}Du}{Q_{L1}}} ,$$

which is itself proportional to the tube current times the duty ratio. This indicates that the tube has a constant sustaining field independent of power level, duty ratio, or loaded Q. Theory indicates[10] that, for this particular tube and cavity, the constant electric field condition should hold for values of the ratio of peak power in megawatts to Q_{L1} less than 0.4. This ratio is proportional to the square of the peak current in the TR tube.

The highest temperature obtainable with the present magnetron was 82°C, with a resonator average power of 25 kw, a duty ratio of 0.003 and a Q_{L1} of 22. The TR tube used was a quartz folded cylinder that had a 0.030-in. gap and was filled with 1 mm of argon. The 3-db recovery time measured was approximately 100 μsec.

In order to carry out tests under conditions of greater dissipation, a 400-watt CW magnetron is being obtained. Although the simulated average power that will be attained with this source will not be significantly higher than that which has been realized with the available pulse source, the duty cycle is higher by a factor of 300. Since, as noted above, the TR dissipation is proportional to the square root of the duty cycle, it is expected that TR dissipation can be increased by $\sqrt{300}$ with the new RF source.

C. E. Muehe
C. W. Jones
C. B. Nelson
A. A. L. Browne

XIII. TEST FACILITY

A. LONG PULSE OPERATION

A VA-87 cathode has been operated at pulse widths of 25, 50, 75 and 100μsec and at a duty cycle of 0.001. At pulse widths greater than 25μsec, however, increasing peak charging current causes a serious sag in power supply voltage and reduces the peak voltage to which the pulse-forming network can be charged. An additional bank of filter capacitors will be installed to overcome this limitation.

Up to this time one VA-87 has been operated at the following levels with a 0.001 duty cycle.

Pulse width in μsec	25	50	75	100
Cathode pulse voltage in kv	90	80	70	68
Cathode pulse current in amps	40	36	30	28
Microperveance	1.5	1.6	1.6	1.6

At these power levels, perveance, gain, and power output are normal. No sag in cathode current due to long pulse has been observed. More extensive operation of this unit is anticipated as soon as this additional filter is obtained.

B. PULSE MODULATOR FOR DEPRESSED COLLECTOR TUBE

Station No. 2, which is capable of 10-kw average, 10-Mw peak at a pulse width of 2μsec has been fitted with an auxiliary transformer, allowing this modulator to be used for both phase-measurement work and the biased-collector tests, and providing a socket to operate experimental VA-87-type cathodes.

W. Janvrin

REFERENCES

1. High-Power Tube Program Semiannual Technical Summary Report to the Advanced Research Projects Agency [U], Lincoln Laboratory, M.I.T. (31 December 1960), ASTIA 250687.
2. W. B. Nottingham, "Design and Properties of the Modified Bayard-Alpert Gauge," Vacuum Symposium Transactions (Pergamon Press, New York, 1954), p. 76.
3. J. Blears, "Measurement of the Ultimate Pressures of Oil Diffusion Pumps," Proc. Royal Soc. A 188, 62 (1947).
4. H. Bruining, Physics and Applications of Secondary Emission (Pergamon Press, New York, 1954).
5. High-Power Tube Program Semiannual Technical Summary Report to the Advanced Research Projects Agency [U], Lincoln Laboratory, M.I.T. (31 December 1959), ASTIA 234064.
6. P. G. R. King, "A 5%-Bandwidth 2.5 Mw S-Band Klystron," Proc. IEE 105B, 813 (May 1958).
7. H. J. Curnow and L. E. S. Mathias, "A Multicavity Klystron with Double-Tuned Output Circuit," S. E. R. L. Technical Journal 8, No. 4, 177 (September 1958).
8. W. L. Beaver, R. L. Jepsen and R. L. Walter, "Wideband Klystron Amplifiers," IRE WESCON Rec. (1957), Part 3, 111.
9. H. W. Bode, Network Analysis and Feedback Amplifier Design (Van Nostrand, New York, 1945).
10. C. E. Muehe, "High Power Duplexers," G-Report 46G-0011 [U], Lincoln Laboratory, M.I.T. (24 May 1961).